Control of Episodic Air Pollution in Utah's Wasatch Front Region Through Investment in Preventative Capital[‡]

Ramjee Acharya[*] *Arthur J. Caplan*[**]

April 6, 2017

Abstract: We address the issue of optimal investment in "preventative capital" to mitigate episodic, mobile-source air pollution events in Utah's Wasatch Front region. We calibrate Berry et al.'s (2015) endogenous-risk model using a unique dataset related to the region's "red air day" episodes occurring over the past decade. Our analysis demonstrates that, under a wide range of circumstances, the optimal steady-state level of preventative capital stock – raised through the issuance of a municipal "clean air bond" that can be used to fund more aggressive mitigation efforts – meets the standard for PM2.5 concentrations with positive social net benefits. We estimate benefit-cost ratios ranging between 5.1:1 and 8.1:1, depending upon trip-count elasticity with respect to the preventative capital stock. These ratios are larger than those reported in Acharya and Caplan (2019) for northern Utah, but still lower than the range generally estimated for the 1990 Clean Air Act Amendments.

Keywords: preventative capital; endogenous risk; $PM_{2.5}$ concentrations; episodic air pollution

JEL Classifications: D62, Q53, Q58

[‡] This study is funded by the Utah Agricultural Experiment Station (UTA0-1334).
[*] Department of Applied Economics, Utah State University, ramjee.acharya@aggiemail.usu.edu.
[**] Professor and corresponding author, Department of Applied Economics, Utah State University, arthur.caplan@usu.edu.

Control of Episodic Air Pollution in Utah's Wasatch Front Region Through Investment in Preventative Capital

Abstract

We address the issue of optimal investment in "preventative capital" to mitigate episodic, mobile-source air pollution events in Utah's Wasatch Front region. We calibrate Berry et al.'s (2015) endogenous-risk model using a unique dataset related to the region's "red air day" episodes occurring over the past decade. Our analysis demonstrates that, under a wide range of circumstances, the optimal steady-state level of preventative capital stock – raised through the issuance of a municipal "clean air bond" that can be used to fund more aggressive mitigation efforts – meets the standard for PM2.5 concentrations with positive social net benefits. We estimate benefit-cost ratios ranging between 5.1:1 and 8.1:1, depending upon trip-count elasticity with respect to the preventative capital stock. These ratios are larger than those reported in Acharya and Caplan (2019) for northern Utah, but still lower than the range generally estimated for the 1990 Clean Air Act Amendments.

Control of Episodic Air Pollution in Utah's Wasatch Front Region

Through Investment in Preventative Capital

1. Introduction

Despite notable achievements made in the control of vehicular emissions during the past 50 years, particulate matter (PM_{10} and $PM_{2.5}$) and ozone concentrations caused by vehicle use in several metropolitan areas of the US continue to exceed National Ambient Air Quality Standards (NAAQS). These exceedances are persistent, episodic, and in certain instances dramatic (Buchmann, 2007; EPHTP, 2017; EPA, 2017; UPHE, 2017; ALA, 2017). An apparent dichotomy between the pace of technological advancement in controlling mobile-source emissions and the prevalence of localized air pollution problems suggests that in those locations currently contending with unhealthy air quality, advancement in technology (e.g., through conversion of a given location's vehicle fleet to a substantial percentage of Tier Three, hybrid, and electric vehicles (EV), i.e., adoption of clean transportation technologies) has not been, and is not likely to be, fast enough for these locations to reach attainment status with $PM_{2.5}$ and ozone NAAQS any time soon (GAM, 2016; J.D. Power, 2010; IEDC, 2013).[1] Ultimately, public policies providing a mix of incentives are needed to (1) motivate behavioral changes in how households utilize their vehicle fleets, and (2) generate the revenue necessary to fund public investments in technologies capable of hastening more immediate mitigation of the pollution problem while simultaneously expediting the transition to cleaner transportation technologies.

[1] The extent of this dichotomy is perhaps best understood via the following statistics. As reported in EPHTP (2017), relative to 1970 models current vehicles produce roughly 80 percent less pollution per mile traveled, even though nationally there are approximately 85 percent more vehicles being driven and 105 percent more miles driven per year (the difference between these latter two percentages is indicative of what has come to be known as the "rebound effect" (Frondel et al., 2008; Sorrell et al., 2009). Concomitant with these vehicle-usage trends are persistent air quality problems in several US metropolitan areas; problems the ALA (2017) estimates negatively impact the health of four in ten people nationwide through what it describes as "unrelenting increases in dangerous spikes in particle pollution".

In this paper we focus on the latter component of the public policy mix (concerning revenue generation), in particular on estimating a region's optimal investment level (e.g., via the issuance of a "municipal clean air bond") in what Berry et al. (2015) and Acharya and Caplan (2019) have labeled "preventative capital", i.e., a capital stock that simultaneously funds more aggressive behavioral-change programs and hastens widespread adoption of cleaner transportation technologies. The specific type of preventative capital we have in mind here is both physical and social infrastructure capable of facilitating implementation of, for example, a seasonal gas tax (c.f., Moscardini and Caplan, 2017), adoption of a congestion-pricing system modified to control for vehicle emissions (c.f., Button and Verhoef, 1998; Beevers and Carslaw, 2005), enhanced public transit (c.f., Nesheli et al., 2017; Horowitz, 1982; Dorsey, 2005), creation and implementation of more persuasive advertising campaigns (c.f., Kassarjian, 1971; Kotler, 2011), subsidization of zero-emission vehicle purchases (c.f., Sierzchula et al., 2014; DeShazo, 2016), etc., each of which alone could help partially control the future occurrence of localized air pollution episodes.[2] Taken together, these types of investments may in fact lead to full control.

Here, we apply Berry et al.'s (2015) endogenous-risk framework – originally developed to estimate optimal investment in disease outbreak prevention and subsequently investigated by Acharya and Caplan (2019) in their study of episodic pollution "outbreaks" in Northern Utah –

[2] Strictly speaking, "prevention" in this case means restraining $PM_{2.5}$ concentrations below the NAAQS during the winter inversion season. By comparison, prevention in Berry et al.'s (2015) model refers to the deterrence of an outbreak of pandemic influenza. As in Acharya and Caplan (2019), our focus in this paper is on estimating the optimal stock of capital – a capital stock which can then be used to fund a variety of programs aimed at mitigating mobile-source pollution – not on how any particular program might subsequently be implemented. Program-by-program assessment is beyond the scope of this study.

to currently one of the nation's worst air quality regions, Utah's Wasatch Front (see Figure 1).[3,4] Episodic air pollution (in particular elevated wintertime $PM_{2.5}$ concentrations) has become an endemic problem in the region (a problem elaborated on in Section 2).[5] In several respects, the Wasatch Front is emblematic of a fast-growing metropolitan area known for its abundance of quality-of-life attributes, such as convenient access to outdoor recreation, ample job opportunities, and pockets of progressive urban growth (WFRC, 2017; Ewing, 2008). In tandem with these amenities, the region's residents express a strong desire for improvements in environmental problems that have festered over time.

According to Envision Utah (2014 and 2013), Wasatch Front residents believe that mitigation of poor air quality should be the state's second highest priority, tied with funding of public education and only slightly behind management of water resources. Survey results indicate that, inter alia, over 60 percent of respondents believe air quality negatively impacts their lives, over 90 percent believe good air quality is integral in maintaining good health, and almost 80 percent believe air quality has worsened in the Greater Wasatch and Northern Utah regions over the past 20 years. Further, residents identify changes in how they transport themselves (i.e., changes in the extent to which they contribute mobile-source emissions), e.g.,

[3] The Wasatch Front is a metropolitan region in the north-central part of Utah. It consists of a collection of contiguous cities stretching along the Wasatch Mountain Range from approximately Nephi in the south to Brigham City in the north. Roughly 80 percent of Utah's population resides in this region (2.5 million people), which contains the state's capital, Salt Lake City and accounts for almost 90 percent of the state's gross state product (Brookings Institution, 2017).

[4] As described in Acharya and Caplan (2019), the application of Berry et al.'s (2015) framework to the problem of episodic air pollution is a natural and pertinent modeling extension given the measurable interplay between exogenous and endogenous risk factors associated with recurring "outbreaks" of elevated pollution events, which in turn induce similarly measurable impacts on human health.

[5] Ignominiously, the Wasatch Front has been ranked the nation's seventh worst region in short-term particulate concentrations by the American Lung Association (ALA) (behind five regions located in California and Fairbanks, Alaska) (ALA, 2017).

telecommuting, ridesharing, use of public transit, reduced idling and unnecessary driving, as being the most beneficial approaches to improving air quality.[6]

[INSERT FIGURE 1 HERE]

The state of Utah and various Wasatch Front regional authorities have not been completely idle in addressing the issue of episodic air pollution outbreaks, or what is commonly known as the occurrence of "red air days" during the winter months. Indeed, several lines of action have emerged over time. On the legislative front, the bipartisan Clean Air Caucus has introduced bills in the state legislature seeking funding for clean-fuel school buses, extension of corporate and individual tax credits for energy-efficient vehicles, and the sponsorship of a variety of competitions aimed to raise awareness of both the problem and actions that can be taken at the household and commercial levels to mitigate it (Alliance for a Better Utah, 2017). Further, emissions testing programs require tests every two years on all vehicles registered in the Wasatch Front region with model years less than six years old, unless the model year is 1967 or older (DMV, 2017). Further, the state actively promotes changes in transportation behavior, e.g., carpooling, use of public transit, teleworking, trip chaining, alternative work schedules, etc., through its Travelwise program (UDOT, 2017). In conjunction with statewide efforts to address the problem, several non-profit organizations advocate and educate for greater awareness of the problem, e.g., Utah Physicians for a Healthy Environment, Breathe Utah, and Heal Utah. As the next section clearly demonstrates, the Wasatch Front's red-air-day problem persists.

This paper reports two sets of findings. First, we estimate a background risk of a red-air day occurring in the Wasatch Front region during the winter inversion season of 12 percent, roughly

[6] Roughly 65 percent of respondents report that they would likely reduce the use of their vehicles if a tax increased the per-gallon price of gasoline by $1.00; 32 percent indicating that they would be very likely to do so (Envision Utah, 2013 and 2014).

four percentage points (25 percent) beneath the 16 percent background risk reported in Acharya and Caplan (2019) for Northern Utah. We also find a positive relationship between the aggregate number of daily vehicle trips taken in the region and the hazard rate associated with exceeding the NAAQS $PM_{2.5}$ concentration threshold of 35 $\mu g/m^3$ on an average winter day. Theoretically expected correlations between exceeding the threshold, on the one hand, and a host of unique weather variables, on the other, are also established. Unlike Acharya and Caplan's (2019) findings for background risk and the hazard rate associated with exceeding the NAAQS in Northern Utah, the determinants of these two risk measures in the Wasatch Front are potentially complicated by what has come to be known as the Great Salt Lake (GSL) effect (Carpenter, 1993; Steenburgh et al., 2000; Alcott et al., 2012). We are able to leverage the weather control variables included in our dataset to implicitly isolate a possible GSL effect on $PM_{2.5}$ concentration levels in Salt Lake County. We find that, all else equal, a GSL effect likely impacts $PM_{2.5}$ concentrations in the county.

Second, we find that the value of the Wasatch Front's optimal, steady-state preventative capital stock is estimated to range from $133 million to $1.6 billion, depending upon the assumed vehicle trip count elasticity with respect to investment in preventative capital. Further, we find that as the region's assumed trip-count elasticity rises the region's optimal daily vehicle trip count (of emitting vehicles) decreases monotonically from approximately 145,000 trips per day to roughly 2,200. At the lowest trip-count elasticity assumed for this study the optimal preventative capital stock results in a concomitant 17 percent decrease in the region's vehicle trip count. The study's largest trip count elasticity corresponds to a 99 percent reduction in daily trip count (which is admittedly conceivable solely via a complete transition of the region's fleet to zero emission vehicles, i.e., effectively zero trips taken with emitting vehicles). As expected,

annual health benefits associated with the concomitant decreases in $PM_{2.5}$ concentrations track the reductions quite closely. Social net benefits are positive for each scenario considered in this study and, unlike in Acharya and Caplan (2019), increase monotonically with trip count elasticity, implying the more responsive is vehicle trip count to investment in preventative capital the larger the social net benefit at the optimal preventative capital stock. Corresponding benefit-cost ratios range between 5.1:1 and 8.1:1, which are larger than those reported in Acharya and Caplan (2019) for northern Utah, but still lower than the range generally estimated for the 1990 Clean Air Act Amendments (EPA, 2011).

As mentioned above, the next section examines the Wasatch Front's red-air-day problem, and also discusses the GSL effect's impact on winter weather patterns, which in turn is believed to alter the impacts of key weather variables on the region's $PM_{2.5}$ concentrations. Section 3 presents a brief review of the relevant economic literature concerning the problem of episodic air pollution. Section 4 presents a condensed version of the Berry et al. (2015) endogenous-risk framework adopted for our subsequent numerical estimation of the region's optimal preventative capital stock.[7] Section 5 discusses the data used in the various empirical analyses underlying our subsequent calibration and numerical simulations of the model. Section 6 presents our econometric results in support of the calibration exercise, and Section 7 presents our numerical results, in particular our estimate of the social net benefit associated with the Wasatch Front's optimal preventative capital stock. Section 8 concludes.

2. The Wasatch Front's Red Air Day Problem

The episodic nature of the Wasatch Front's red air day problem is depicted most tellingly by the various panels of Figure 2 and associated statistics presented in Table 1. Figure 3 shows that

[7] A fuller version of the Berry et al. (2015) model is provided in Acharya and Caplan (2017).

elevated $PM_{2.5}$ concentrations are clearly a wintertime phenomenon along the Wasatch Front; on average the mass of concentrations occur between the months of December – February.

[INSERT FIGURES 2 AND 3 AND TABLE 1 HERE]

As indicated by the first row of time-series graphs presented in Figure 2, Salt Lake County's $PM_{2.5}$ concentrations spiked above the NAAQS of 35 $\mu g/m^3$ (horizontal orange line) more frequently and with greater intensity during the 2003-2004 winter inversion season than during the previous season. Utah and Weber Counties similarly experienced more frequent and intense red air day episodes during the 2006-2007 and 2009-2010 inversion seasons, respectively, relative to their previous seasons. As shown in Table 1, the median percentage of winter days (December – February) exceeding the NAAQS threshold of 35 $\mu g/m^3$ across the Wasatch Front for our study period of 2002-2012 was 18 percent. The annual percentages show no apparent declining or inclining pattern over the course of our study period.

As discussed at length in Acharya and Caplan (2019) and Moscardini and Caplan (2017), $PM_{2.5}$ concentrations consist of dust and smoke particles, which in the case of the Wasatch Front emanate primarily from vehicle emissions (50 percent) and area sources (35 percent) (Whiteman et al., 2014). Wintertime inversions that trap these particles occur as the temperature at ground level falls beneath the temperature at higher elevations, immobilizing the pollutants at the surface (UDEQ, 2016b). More specifically, as elevation rises temperature gradually decreases. Given conducive humidity, snowfall, snow depth, and wind-speed conditions, descending warm air creates an inversion layer. Within this layer, temperature increases with increasing elevation, constituting the reverse of normal air patterns. The inversion layer traps $PM_{2.5}$ concentrations between geologic barriers which, in the case of the Wasatch Front, are the Wasatch and Oquirrh Mountain Ranges.

Short-term exposure to elevated $PM_{2.5}$ concentrations is linked to increased hospital admissions and emergency department visits for respiratory effects, such as asthma attacks, as well as increased respiratory symptoms, such as coughing, wheezing and shortness of breath. In addition, short-term exposure is linked to reduced lung function in children and in people with asthma. Long-term exposure to elevated $PM_{2.5}$ concentrations can cause premature death due to heart and cardiovascular disease associated with heart attacks and strokes. Some studies suggest that long-term exposure can cause cancer as well as harmful developmental and reproductive defects, such as infant mortality and low birth weight (EPA, 2016b; Dockery et. al, 1993; Pope et. al, 1995; Pope, 1989).

As pointed out by Moscardini and Caplan (2017), during a typical inversion episode anywhere from 60 to 85 percent of all $PM_{2.5}$ is created by secondary particulate formation (UDEQ, 2016a). Secondary particulate formation occurs when precursor emissions of nitrogen oxides (NOx), sulfur oxides (SOx), and especially volatile organic compounds (VOCs) from vehicle emissions react and combine in the atmosphere to create concentrations of $PM_{2.5}$ (UDEQ, 2016a). A host of weather variables contribute to the duration and intensity of elevated $PM_{2.5}$ concentrations during the winter inversion season, including temperature, humidity, snowfall, and snow depth levels, wind speed, and, as we are able to isolate in Section 6, motor vehicle use, which as mentioned above contributes the majority of the Wasatch Front's $PM_{2.5}$ precursor emissions. The resulting emergence of a typical red air day episode along the Wasatch Front is therefore governed by the same constituents as those occurring in Northern Utah (Acharya and Caplan, 2019). However, as mentioned in Section 1 the Wasatch Front's process is further tempered by what is believed to be significant GSL effect snowstorms occurring each winter (Carpenter, 1993; Steenburgh et al., 2000; Alcott et al., 2012).

Although difficult to predict, lake-effect snowstorms are produced by boundary-layer and mesoscale air circulations associated with localized heating over lake surfaces and sufficient low-level, relative humidity conditions (Alcott et al., 2012). Localized heating is accentuated by the lake's shallow depth, high reflectivity, and hyper-saline composition, which together with the Front's steep topographic barriers and heavily populated urban corridor can occasionally induce strong lake-land temperature contrasts leading to higher snowfall events (or solitary snow bands) than would otherwise be the case (historically averaging roughly one-two per month during the Wasatch Front's winter inversion season) (Steenburgh et al., 2000 and Alcott et al., 2012). Because of their relatively infrequent occurrences, we do not expect lake effects to drastically alter the signs and statistical significance levels of the weather control variables included in our regressions relative to those used in Acharya and Caplan (2019) for Northern Utah. However, slight differences in the marginal effects of these particular control variables on $PM_{2.5}$ concentrations would not be overly surprising.[8] In Section 6.2 we attempt to isolate the lake effect's possible impacts on the Wasatch Front's wintertime $PM_{2.5}$ concentrations in the context of our particular dataset.

3. Literature Review

The current study is patterned after our previous analysis of Northern Utah's red air problem – analysis resulting in empirical estimation of that region's optimal preventative capital stock under a variety of conditions (Acharya and Caplan, 2019). In specific, Acharya and Caplan (2019) estimate a positive relationship between the aggregate number of vehicle trips taken in Northern Utah and the region's hazard rate associated with exceeding the NAAQS $PM_{2.5}$ concentration threshold of 35 $\mu g/m^3$ on an average winter day. Theoretically expected

[8] As Alcott et al. (2012) point out, the unavailability of lake temperature data precludes statistical identification of lake effects with any great degree of precision and reliability.

correlations between exceedances of the threshold, on the one hand, and a host of unique weather variables (in particular snow depth, temperature gradient, and snowfall and humidity levels), on the other, are reported.

The authors find that the value of Northern Utah's optimal, steady-state preventative capital stock ranges from $4 million to $14 million depending upon the assumed vehicle trip count elasticity with respect to investment in preventative capital (with corresponding amortized annual values ranging from $330,000 to $1.13 million per year, respectively). Further, they find that although the region's optimal vehicle trip count (of emitting vehicles) decreases monotonically from approximately 45,000 trips per day to just under 3,000 as trip-count elasticity rises, the corresponding optimal preventative capital stock exhibits a non-monotonic relationship with the trip-count elasticity. The value rises from just over $4 million with an elasticity of 0.1 (corresponding to a 13 percent decrease in the region's vehicle trip count) to just over $14 million for an elasticity of 0.8 (corresponding to a 93 percent trip-count reduction).

Acharya and Caplan (2019) find that annual benefits associated with the concomitant decreases in $PM_{2.5}$ concentrations in northern Utah track the reductions quite closely. Social net benefits increase monotonically with trip count elasticity, indicating that the more responsive is vehicle trip count to investment in preventative capital, the larger the social net benefit associated with the optimal preventative capital stock. Benefit-cost ratios range from 3.1:1 at the lowest elasticity level to 11.3:1 at the highest elasticity level. These ratios are lower than EPA's (2011) estimated range for the 1990 Clean Air Act Amendments of between 3:1 and 90:1.

The present study extends Acharya and Caplan's (2019) framework of analysis to the state of Utah's most populous and economically dynamic region; a region consisting of multiple counties (i.e., political jurisdictions) with boundaries that are, at least to some extent, ignored by the

weather patterns and mobile-source emissions that engender the region's red air day episodes during winter inversion season. As a result, the econometric analyses underscoring our numerical estimation of the region's optimal preventative capital stock must simultaneously account for county-level distinctions in the data (i.e., data categorized by existing political jurisdictions) and potential cross-sectional dependence at the county level (due to cross-county commonalities in weather patterns and emissions) that might otherwise bias the empirical models' estimates of exogenous background risk and the hazard associated with county-level vehicle trips (elaborated on in Section 6).

Moscardini and Caplan (2017) and Cropper et al. (2014) are the most recent studies to investigate market-based policies to control episodic air pollution attributable to vehicle emissions.[9] In their study of Northern Utah, Moscardini and Caplan (2017) find that, on average, a one-percent decrease in county-level trip count results in a 0.75 percent reduction in $PM_{2.5}$ concentrations, all else equal. Further, a one-percent increase in gas price (in response to the imposition of a seasonal gas tax) is correlated with a 0.31 percent reduction in vehicle trips. The authors estimate substantial seasonal social net benefits associated with the imposition of a seasonal gas tax. Their deadweight loss (DWL) estimate associated with the tax ranges from $2.5 million - $ 4 million, weighed against a median social benefit estimate of $19.6 million arising from reduced healthcare costs accompanying reduction in $PM_{2.5}$ concentrations.

Cropper et al. (2014) similarly assess the potential of a mobile-source permit program to control ground-level ozone concentrations in Washington, DC. The authors' estimate that their

[9] Henry and Gordon (2003), Cummings and Walker (2000), and Cutter and Neidell (2009) assess the impact of voluntary driving restrictions in the US. In Europe, studies have assessed the impacts of daily congestion fees in Stockholm, Sweden; London, England; and Milan, Italy (Carnovale and Gibson, 2013; Button and Verhoef, 1998; Phang and Toh, 2004; Anas and Lindsey, 2011), and the creation of low-emissions zones in Germany (Wolff, 2014). Mandatory driving restrictions have recently been implemented in Sao Paulo, Brazil and Bogota, Colombia (Zhang et al., 2016), Santiago, Chile (Gallego et al., 2013), and San Jose, Costa Rica (Osakwe, 2010).

proposed scheme would remove one million vehicles from the road during high-ozone days, resulting in a corresponding reduction in NO_x emissions of 30 tons per day and generating an estimated $111 million annually in government revenue, even in the face of non-compliance. Taken together, Moscardini and Caplan (2017) and Cropper et al. (2014) are suggestive of the potential that market-based incentives have to mitigate episodic air pollution problems attributable primarily to mobile-source emissions. As mentioned in Section 1, the public expenses associated with planning for and implementing these types of incentives, along with additional investments in physical and social capital, are precisely what investments in preventative capital could conceivably cover.

4. Berry et al. (2017) Endogenous Risk Model

As in Acharya and Caplan (2019), we adopt Berry et al.'s (2015) endogenous-risk model of disease outbreaks to estimate the optimal preventative investment rate and capital stock to control episodic red air days in the Wasatch Front. Accordingly, we let B represent (constant) annual region-wide GDP and $z(t)$ represent preventative investment in time period t. Following an "outbreak" of a red air day episode, the region experiences cumulative environmental costs associated with that outbreak represented by $D(t)$, which can diminish over time.

Following Berry et al. (2015), the Wasatch Front's maximization problem to determine optimal investment in preventative capital can be written as,

$$\max_{z(t)} W = \int_0^{\infty} [B - z(t) + \Psi(N(t), R(t)J]e^{-rt-y(t)}\, dt$$

$$s.t.\ \ \dot{N}(t) = z(t) - \delta N(t),\ \dot{R}(t) = \sigma\big(R(t)\big),\ \dot{y}(t) = \Psi\big(N(t), R(t)\big), \qquad (1)$$

$$N(0) = N_0\,,\ R(0) = R_0\,,\ y(0) = 0,\ z(t) \geq 0\,,$$

where, using B and $D(t)$ as defined above, $J = \int_0^\infty \big(B - D(t)\big)e^{-rt}dt$, i.e., J represents the present value of ex post net benefits given a red air day episode has occurred. Function $\Psi(N(t), R(t))$ (with curvature conditions $\Psi_N < 0, \Psi_R > 0, \Psi_{NN} > 0, \Psi_{NR} > 0$, and $\Psi(N(t), 0) = 0$) represents the region's episodic hazard function, or instantaneous probability of a red air day occurring (described in more detail in Section 4.2), $y(t)$ denotes cumulative hazard function $\int_0^t \Psi(N(v), R(v))dv$, r is the social discount rate, $N(t)$ the level of preventative capital at time t (given initial level N_0), $R(t)$ the exogenous background risk of a red air day episode occurring at time t (given initial risk level R_0), and δ denotes the depreciation rate of the preventative capital stock. Net investment in preventative capital in period t is therefore defined as $\dot{N}(t) = z(t) - \delta N(t)$, and the evolution of background risk over time is denoted by function $\sigma\big(R(t)\big)$.

As in Acharya and Caplan (2017), we empirically estimate the region's steady-state level of background risk, R^{ss} via probit regression analysis (following Greene, 2012, and Long and Freese, 2006), in our case using a panel dataset (described in more detail in Section 5). Hazard function $\Psi(N(t), R(t))$ is also estimated based on this dataset following Greene (2012) and Cleves et al. (2010). To link the preventative capital stock $N(t)$ with daily trip counts ($TC(t)$) within hazard function $\Psi(N(t), R(t))$, we assume a constant-elasticity formulation,

$$\ln\big(TC(t)\big) = A - c\ln\big(N(t)\big) \qquad (2)$$

where $c \in (0.1,1)$ represents the (absolute value) of trip-count elasticity with respect to preventative capital stock, and constant A is calibrated from (2) assuming median trip count for the region and $N(0)$ = \$20 million.[10]

[10] The range of trip-count elasticities adopted for this study represent a range of possible behavioral responses of drivers to different scales of investment in preventative capital. Since $N(0)$ is chosen arbitrarily for this analysis, we

As discussed in Acharya and Caplan (2019), despite the absence of studies looking specifically at the relationship between vehicle usage and investment in preventative capital stock, we can nevertheless appeal to a related literature for comparable estimates. For example, APTA (2014) consider aggregate savings in vehicle operating and fuel costs associated with reduced vehicle usage in response to expanded capital investment in public transport. Their elasticity estimates range from a high of 0.56 to a low of 0.48. Similarly, Litman's (2011) assessment of the Transport for London's investment in a video camera network to manage congestion in Central London suggests an elasticity of roughly 0.2. Litman (2017) reports an average elasticity of transit use with respect to transit service frequency of 0.5, and elasticities with respect to service expansion ranging between 0.6 and 1. These findings therefore suggest that our chosen range for parameter c is consistent with what empirical evidence is available.

As Berry et al. (2015) show, the solution to maximization problem (1) can be written as,

$$\mathrm{z(N,R)} = \delta N + \left[-\rho(N,R) - \frac{\Psi_R(N,R)}{\Psi_N(N,R)}\left(1 - \varepsilon_\Psi \frac{\gamma(N,R)}{N}\right)\right]\frac{\sigma(R)}{1-\gamma_N(N,R)}, \quad (3)$$

where $\varepsilon_\Psi = |\Psi_{RN}(N,R)(N/\Psi_R(N,R))|$ is the (absolute value) of the elasticity of the hazard's response to R with respect to a change in N. This elasticity measures the relative endogeneity of risk associated with a red air day episode, i.e. the degree to which the impacts of background risk on the hazard rate can be managed via N. The larger the elasticity, the more effective is preventative capital (Berry et al., 2015). Similarly, $\gamma(N,R) = \frac{r+\delta+\Psi(N,R)}{-\Psi_N(N,R)}$ and $-\rho(N,R) = \frac{B-\delta N-rJ-[r+\Psi(N,R)]\gamma(N,R)}{\sigma(R)}$.

sensitize the analysis to alternative values of $N(0) \in [\$10 \text{ million}, \$20 \text{ million}]$. This range of values is based on the $N(0)$ values assumed by Acharya and Caplan (2019) for Northern Utah, scaled according to relative regional gross domestic products (GDPs) across the two regions – the Wasatch Front's economy is roughly 20 times the size of Northern Utah's (UEC, 2015).

As discussed in Berry et al. (2015), if the expression in the square bracket in equation (3) is positive then net preventive investment (i.e. $z - \delta N$) increases with background risk. The first term in brackets, $-\rho(N,R)$, is the shadow value of increasing background risk, which is positive, i.e., the larger the background risk, the larger is the net investment required to prevent an episodic outbreak. The ratio $\frac{\Psi_R(N,R)}{\Psi_N(N,R)}$ represents the rate of substitution of N for R in managing the hazard rate, which is negative.

To determine the optimal steady-state preventative capital stock, we follow Berry et al. (2015) and Acharya and Caplan (2019) in utilizing the theoretical model's two steady-state equations,

$$\dot{N}(t) = z(t) - \delta N(t) = 0 \tag{4}$$

$$\sigma\big(R(t)\big) = R(t)(1 - \tfrac{R(t)}{R^{ss}}) = 0. \tag{5}$$

Combining equations (3) and (4) results in

$$\Big[-\rho(N,R) + \tfrac{\Psi_R(N,R)}{-\Psi_N(N,R)}\Big(1 - \varepsilon_\Psi \tfrac{\gamma(N,R)}{N}\Big)\Big]\tfrac{\sigma(R)}{1-\gamma_N(N,R)} = 0. \tag{6}$$

Next, equations (5) and (6) are solved simultaneously to obtain optimal steady-state preventative capital stock N^{ss}. Lastly, as in Berry et al. (2015) and Acharya and Caplan (2019) we use the law-of-motion equation for $\sigma(t)$ (equation (5) now set equal to zero) to explore the dynamics of increasing background risk over time. Letting initial background risk be relatively close to zero, in particular $R(0) = 0.005$, and using $\sigma(t)$ to update $R(t)$ over time, the background risk (at the end of) period 1 is given by $R(1) = R(0) + \sigma(0)$, where $\sigma(0) = R(0)(1 - \frac{R(0)}{R^{ss}})$, and similarly for $R(2)$, $R(3)$ and so on. The corresponding $z(t)$ values can then be calculated for given N^{ss} using equation (3).

5. Data

The data used in our empirical analyses are compiled from several different sources. Each variable in the dataset consists of a daily time step for the years 2002 – 2012 for each of the three counties (Salt Lake, Weber, and Utah) comprising the Wasatch Front region.[11] Since the problem addressed in this study occurs seasonally each year (from December – February) we restrict the dataset to these three months. We utilize $PM_{2.5}$ concentration measurements from two monitoring stations in Weber County (located in the cities of Ogden and Harrisville), five stations from Salt Lake County (located at Hawthorne, Great Salt Lake, Great Salt Lake beach Marina, Magna, and Rose Park), and three stations from Utah County (located in the cities of Lindon, North Provo and Spanish Fork) (UDEQ 2016).

Relevant weather variables – consisting of the temperature gradient between high and low points in each county, wind speed, humidity, snow depth and snowfall level – were obtained from the Weather Underground and the Utah Climate Center (Weather Underground, 2016; Utah Climate Center, 2017). Lastly, county-level, daily vehicle trip count data was averaged across 13 Automatic Traffic Recorder (ATR) stations for Salt Lake County, nine ATR stations for Utah County, and two ATR stations for Weber County.[12]

Summary statistics and variable definitions for the specific variables used in the ensuing analyses are presented in Table 2. As indicated, the median number of daily vehicle trips in the Wasatch Front region, *TC*, is approximately 175,000. The region's average daily $PM_{2.5}$

[11] The Wasatch Front consists of five counties total, including Davis and Box Elder Counties. Unfortunately, weather and trip count data for these two counties are either non-existent (Box Elder) or inconsistent (Davis) for our study period. $PM_{2.5}$ concentrations, vehicle trip counts, and the weather control variables for the three counties used in this study are reported by their various sources on an hourly basis. For the ensuing analyses we use the associated daily hourly averages.

[12] As opposed to Acharya and Caplan (2019), who use maximum number of daily trips across ATR stations as their measure of trip count, we use average daily trip count per county across respective ATR stations due to the relatively wide geographic spreads of station locations in each of our three counties.

concentration during the three winter months is approximately 17 $\mu g/m^3$, while the mean value for indicator variable *Y* (indicating whether a given day's $PM_{2.5}$ concentration exceeds the NAAQS threshold of 35 $\mu g/m^3$) is 0.12, implying that, on average, the NAAQS were exceeded 12 percent of the time during the winter months of our study period in the Wasatch Front. The remaining variables – *TEMP*, *WIND*, *HUMIDITY*, *SNOWFALL*, *HUMWIND* and *SNOWDEPTH* – denote the daily temperature difference in each county between mountain peak and corresponding valley floor, wind speed, humidity level, snowfall level and snow depth, respectively. According to Gillies et al. (2010), Wang et al. (2015), Silcox et al. (2012), and Whiteman et al. (2014), temperature gradient is a key determinant of winter-inversion conditions, along with snowfall level and snow depth.

[INSERT TABLE 2 HERE]

According to UDEQ (2018), a snow-covered valley floor reflects rather than absorbs heat from the sun, preventing normal mixing of warm and cold air and exacerbating the accumulation of $PM_{2.5}$ concentrations in the atmosphere. The deeper the snow depth the more heat is absorbed and the greater the positive effect on concentrations. Snowfall is coincident with lower air pressure, which in turn negatively affects $PM_{2.5}$ concentrations, all else equal. Calm winds reduce the mixing of warm and cold air and can also negatively affect concentrations, while higher levels of relative humidity are associated with higher concentration levels. We investigate in Section 6 the extent to which these weather variables determine the Wasatch Front's background risk of a red air day occurrence, as well as the hazard associated with initiation of a red air day episode.

6. Empirical Analyses

In this section we present the empirical models used to estimate our data, along with the corresponding econometric results. We first estimate a panel Probit model using a subset of the

variables contained in Table 2 in order to derive a mean estimate of the Wasatch Front's steady-state level of background risk, R^{ss}, described in Section 4. We then derive an estimate of the region's episodic hazard function $\Psi(N(t), R(t))$, also described in Section 4. As shown in Section 7, estimates of R^{ss} and $\Psi(N(t), R(t))$ are crucial factors in our subsequent numerical simulations determining the region's optimal steady-state preventative capital stock N^{ss} and corresponding investment in preventative capital, z^{ss}.

6.1. Probit Analysis of Background Risk

Empirically, we can represent R^{ss} as the average probability of a red air day occurring in the Wasatch Front during the winter months.[13] Following Green (2018, Section 17.3) and Long and Freese (2014, Section 5.1), this probability can be estimated according to,

$$Pr(Y = 1|\boldsymbol{X}) = \int_{-\infty}^{\boldsymbol{X}'\boldsymbol{\beta}} \phi(t)dt = \Phi(\boldsymbol{X}'\boldsymbol{\beta}), \tag{7}$$

where variable Y is as defined in Table 2, the functions $\phi(.)$ and $\Phi(\boldsymbol{X}'\boldsymbol{\beta})$ represent the standard normal and cumulative standard normal distribution functions, respectively, and subscript t represents a given day. Matrix $\boldsymbol{X}$ contains daily observations on the model's covariates (a subset of the variables defined in Table 2), and $\boldsymbol{\beta}$ is the corresponding vector of parameters to be estimated from the data. The marginal effect of covariate $x_i \in \boldsymbol{X}, i = 1, \ldots I$, is then calculated using maximum-likelihood estimation as

$$\frac{\partial(Pr(Y_t = 1|\boldsymbol{X}))}{\partial x_i} = \phi'(\boldsymbol{X}'\boldsymbol{\beta})\boldsymbol{\beta_i}, \tag{8}$$

[13] As in Acharya and Caplan (2019), we proxy for background risk with the probability of a red air day occurring rather than merely the probable occurrence of a temperature inversion (as described in Section 2) because our data suggests that roughly 11 percent of red air days are not coincident with an inversion. Further, we do not consider *TC* as an omitted variable from this model because it is uncorrelated with the remaining variables. As we discuss in Section 6.3, *TC* can instead be instrumented with either a weekday dummy or a series of day-of-the-week dummies.

where $\phi'(\boldsymbol{X}'\boldsymbol{\beta})$ is the marginal density function associated with $\Phi(\boldsymbol{X}'\boldsymbol{\beta})$ (Green, 2018, Section 17.3).

Steady-state background risk, R^{ss}, is then computed as the average of predicted probabilities of a red air day occurrence across the three counties using a population-averaged panel probit model (STATA, 2017). We chose the population-averaged estimator due to our exclusive use of environmental variables (i.e., the weather controls and $PM_{2.5}$ concentration levels) to explain background risk in the model; variables exhibiting a relatively large degree of cross-sectional dependence across counties (the respective panels in our dataset) due to their natural lack of adherence to what are solely political boundaries (Neuhaus, et al., 1991).

As shown in Table 3 (and as expected given the county's close geographical proximities to each other and thus shared (on average) meteorological conditions), the estimated county-level probabilities of red air day occurrences are closely related. Averaged across the three counties, the Wasatch Front's background risk is estimated to be 12 percent, a full 4 percentage points (or 25 percent) beneath the background risk of 16 percent estimated by Acharya and Caplan (2019) for Northern Utah over the same timeframe. This difference may be at least partially explained by the GSL lake effect described in Section 2; a difference we explore more fully in Section 6.2 with respect to the model's estimated marginal effects. The estimated coefficients, their corresponding marginal effects, and goodness of fit measures for our population-averaged model are also provided in Table 3.[14] With respect to the model's overall fit, actual red air days (non-red air days) are correctly predicted 57(98) percent of the time.

[INSERT TABLE 3 HERE]

[14] In addition to the random-effects version of the model, we ran a host of other specifications including different sets of explanatory variables. Results for these models are available from the authors upon request. We used STATA version 14.1 for our regression analyses.

Further, we find that *TEMP* exhibits a positive and statistically significant effect on the probability of a red air day occurrence. All else equal, the higher the temperature gradient between the region's higher elevations and valley floor, the higher the probability of a red air day occurrence. This result conforms with Gillies et al. (2010), Silcox et al. (2012), and Wang et al. (2015). However, the magnitude of effect is lower than that for Northern Utah (Acharya and Caplan, 2019). The marginal effect for $LagPM_{2.5}$ is also positive, as expected, and stronger than that for Northern Utah. Similarly as anticipated, variables *HUMWIND* and *SNOWFALL* are negative and statistically significant, aligning with Whiteman et al.'s (2014) earlier findings for the Wasatch Front region.[15] However, the marginal effects associated with *HUMIDITY* and *SNOWDEPTH* are both statistically insignificant, unlike in Utah's northern region. Overall the model does a better job of predicting non-red air days (98 percent of the time) than red air days (57 percent of the time). The model is estimated with White (1980) robust standard errors, which controls for potential within-panel autocorrelation (Arellano, 2003).

We also ran the population-averaged model in Table 3 without $LagPM_{2.5}$ as a regressor in order to assess the impact on the remaining regressors' coefficient estimates (as a test of $LagPM_{2.5}$'s potential endogeneity) and standard errors (as a test of potential serial autocorrelation). The results were qualitatively very similar – the magnitudes of the marginal effects for *TEMP* and *HUMIDITY* both increased, but those for *HUMWIND, SNOWFALL*, and *SNOWDEPTH* stayed roughly the same. The estimate for R^{ss} increased by roughly 2.5 percentage points to 14.4 percent. Interestingly, a random-effects version of the model without $LagPM_{2.5}$ included as a regressor produces marginal effects that are very similar to those

[15] As described in Acharya and Caplan (2019), slight breezes stimulate the evaporation of water, leading to increases in humidity. Thus, we expected *HUMWIND* to exhibit a negative relationship with $PM_{2.5}$. *WIND* was included in an earlier specification and found to be statistically insignificant.

estimated by the population-averaged model, but the corresponding estimate of R^{ss} decreases only by roughly one percentage point to 10.7 percent.

6.2 A Great Salt Lake Effect on Salt Lake County's $PM_{2.5}$ Concentrations

According to Carpenter (1993), Alcott et al., (2012), and Steenburgh et al., (2000) (henceforth referred to as CAS), the GSL effect specifically impacts the Salt Lake Valley, which is located entirely within the boundaries of Salt Lake County. Hence, to the extent that it is implicitly captured by the weather control variables included in our dataset, we may be able to distinguish the GSL effect's potential impacts on $PM_{2.5}$ concentration levels in Salt Lake County relative to the absence of impacts experienced in Utah and Weber Counties.[16] Conditions unique to Salt Lake County could in turn be driving the econometric results reported for the Wasatch Front as a whole in Section 6.1, particularly regarding the absence of a statistically significant *SNOWDEPTH* effect on the probability of a red air day occurrence. CAS's findings suggest that a weakened *SNOWDEPTH* effect could in fact be a consequence of amplified interactive effects between combinations of *HUMIDITY*, *TEMP*, and *SNOWFALL* during periodic occurrences of the lake effect.

To test for the potential impact of the GSL effect on $PM_{2.5}$ concentration levels in Salt Lake County, we ran a series of panel-data models with (1) controls for both the endogeneity of $LagPM_{2.5}$ and potential within-panel autocorrelation, (2) our full set of weather variables, and (3) a series of weather interaction terms specifically targeting the impact of Salt Lake County's weather conditions on its $PM_{2.5}$ concentrations.[17] Table 4 contains our results for two different

[16] We are unfortunately precluded from explicitly controlling for specific lake-effect occurrences in our dataset. Carpenter's (1993) and Steenburgh et al.'s (2000) study periods precede ours, while Alcott et al.'s (2012) overlaps solely with our study's first six years. We know of no other studies documenting the GSL effect during our study period, thus we are unable to explicitly control for the effect on the specific days in which it occurred.

[17] Each model is estimated with White (1980) robust standard errors, which controls for potential within-panel autocorrelation (Arellano, 2003). The R^2 (overall) is reported for each model as a measure of explained total

specifications. Following Moscardini and Caplan (2017) and Acharya and Caplan (2019), Model 1 controls for *TC*'s potential endogeneity using as instruments weekday dummy variables for Monday – Friday.[18] Model 2 provides specific controls for potential endogeneity in both *TC* and $LagPM_{2.5}$, where the instrument for the latter is the second lag of $PM_{2.5}$ (Becketti, 2013). Model 2 is our preferred specification, however the results across the two models are qualitatively very similar. The ensuing discussion is therefore general to both models.

[INSERT TABLE 4 HERE]

As anticipated, $LagPM_{2.5}$, *TC*, *TEMP*, *HUMIDITY*, and *SNOWDEPTH* each exhibit positive and statistically significant relationships with $PM_{2.5}$ across the Wasatch Front on average. To the contrary, the effects of *HUMWIND, SNOWFALL,* and an annual time trend (*YR_T*) on $PM_{2.5}$ are both negative – the latter effect indicating that, all else equal, $PM_{2.5}$ concentrations along the Wasatch Front have been diminishing over time. Interestingly, the coefficient for *WIND* is positive and statistically significant across both models. Our hypothesis concerning this unexpected result is that increasing (prevailing westerly) wind levels in a given county affect both wind and $PM_{2.5}$ conditions in neighboring counties in potentially unpredictable ways. One possible theory is that as wind levels rise across the Wasatch Front, $PM_{2.5}$ concentrations partially transgress county boundaries in the westerly direction, adding in net to accumulated concentrations in any given neighboring county.

The dummy variable for Salt Lake County (*SLC*) is positive and statistically significant, indicating some evidence for the hypothesis that, all else equal, $PM_{2.5}$ concentration levels are higher in SLC than in Utah and Weber Counties. In addition to this overall average effect of

variation. For comparison purposes the Adjusted R^2 measure from pooled OLS equals 0.75. The Wald χ^2 statistics indicate that we can reject the null hypothesis of jointly insignificant explanatory variables.

[18] Fixed-effects outperformed random-effects for each model reported here based on standard Breusch and Pagan (1980) LM and Hausman (1978) χ^2 tests.

SLC's concentration levels within the Wasatch Front, the array of SLC-specific interaction terms reported in Table 4 provide our window into the nuances of a GSL effect in the Salt Lake Valley that may be driving this divergence between SLC and the rest of the Front. Two-way interaction terms potentially controlling for a GSL effect on SLC's $PM_{2.5}$ concentrations include *SLC_TEMP*, *SLC_SNOWFALL*, *SLC_SNOWDEPTH*, and *SLC_WIND*. All else equal, SLC's temperature gradient (*SLC_TEMP*) and wind (*SLC_WIND*) effects are attenuated (less positively related to its $PM_{2.5}$ concentrations) than are the same effects in Utah and Weber Counties. To the contrary, the negative effects of snowfall and positive effects of snow depth on the Front's $PM_{2.5}$ concentrations are both exasperated in SLC, as indicated by the negative(positive) coefficient estimates for *SLC_SNOWFALL* and *SLC_SNOWDEPTH*, respectively.

The complexity of underlying weather conditions contributing to the GSL effect – as described in CAS – are perhaps best captured by our three-way interaction terms *SLC_TEMP_HUMIDITY* and *SLC_TEMP_SNOWFALL*. The respective positive coefficient estimates (statistically significant solely in Model 2 for the latter) suggests that a GSL effect in SLC may at least be partially offsetting the negative impacts that interacted temperature-gradient and humidity (*TEMP_HUMIDITY*) and snowfall (*SNOWFALL_TEMP*) conditions otherwise have on the Wasatch Front's average $PM_{2.5}$ concentrations. Taken together, this suite of SLC-specific, two- and three-way interaction terms therefore suggests that a GSL effect may in fact influence variation in SLC's $PM_{2.5}$ concentrations, and thus our average estimates of weather impacts on the Wasatch Front's concentrations as well.

6.3. Survival Analysis

As in Acharya and Caplan (2019), we let $G(\boldsymbol{X}(t))$ represent the Wasatch Front's probability of an episodic outbreak of red air days in period t, where $\boldsymbol{X}(t)$ is a vector of covariates from Table

2. The corresponding survival function is written as $S(t) = 1 - G\big(\boldsymbol{X}(t)\big)$, and the hazard function $\Psi(\cdot)$ solves for the probability of an episodic outbreak given its non-occurrence prior to t (see Acharya and Caplan (2019) for further interpretation of what $\Psi(\cdot)$ represents in the context of our particular framework). Following Berry et al. (2015), we define the hazard function in general as,

$$\Psi\big(\boldsymbol{X}(t), R(t)\big) = R(t) lim_{\Delta t \to 0} \left(\frac{outbreak\ in\ (t,t+\Delta t) | no\ outbreak\ at\ t}{\Delta t}\right) = \frac{R(t) g(\boldsymbol{X}(t))}{S(\boldsymbol{X}(t))}, \qquad (9)$$

where $g(\cdot)$ is the probability density function (pdf) of $G(\cdot)$ and $R(t)$ again represents exogenous background risk. Conditioning $\Psi\big(\boldsymbol{X}(t), R(t)\big)$ on $N(t)$ post-estimation requires that a functional relationship be assumed between $TC(t)$ (which is a member of $\boldsymbol{X}(t)$) and $N(t)$. As discussed previously in Section 4, we apply a double-log specification of this relationship (refer to equation (2)) in our ensuing numerical analysis in Section 6.4.

We tested several standard parametric panel models for the survival analysis – exponential, Weibull, and the semi-parametric Cox model. The Weibull hazard function – defined specifically as $\Psi\big(\boldsymbol{X}(t), R(t)\big) = R(t) p t^{p-1} \exp(\boldsymbol{X}(\boldsymbol{t})' \boldsymbol{\beta})$, where parameter p represents the function's shape parameter and all other terms are as previously defined (Cleves et al., 2010) – performed best in fitting our data.[19] As in Acharya and Caplan (2019), the occurrence of a series of daily $PM_{2.5}$ concentrations above the threshold 35 μg/m³ level in the region is considered an event in this study. For this analysis, a count-data variable must also be specified (Cleves et al., 2010, Section 3.1); ours is defined as follows. After the first episodic outbreak, for example in December, we begin the count within a window during which $PM_{2.5}$ concentrations steadily increase,

[19] The Weibull hazard function exhibits the appealing property of increasing hazard over time for shape parameter $p > 1$.

consecutively day-after-day, until the next episode occurs. Similar counts are then taken between successive episodes.

Results for our empirical estimation of the hazard function's determinants are provided in Table 5, where we present two versions of the Weibull panel model. In Model 1, potential endogeneity in the *TC* variable is controlled for with separate weekday dummy variables for Monday - Friday, as in Moscardini and Caplan (2017) and Acharya and Caplan (2019) (with *TC** representing the instrumented version of *TC*). The presence of endogeneity in the relationship between $PM_{2.5}$ concentrations and *TC* is confirmed via a standard Durbin-Wu-Hausman test (Davidson and MacKinnon, 1993). For comparison purposes Model 2 ignores potential endogeneity in the trip count variable, thus *TC** represents natural log of trips in this model.

[INSERT TABLE 5 HERE]

The coefficients for TC^* in both models are positive, indicating that on average an increase in the Wasatch Front's vehicle trip count increases the hazard of a red air day occurring. However, this effect is statistically insignificant in Model 1 after controlling for potential endogeneity.[20] The coefficients for *TEMP* and *SNOWFALL* are each of the expected signs, and are statistically significant; *SNOWDEPTH* is statistically insignificant in both model specifications.[21] Since shape parameter *p* is greater than 1 in each model, the hazard of a red air day occurring in the Wasatch Front is estimated to be monotonically increasing over the course of any given window

[20] The statistical insignificance of *TC** after controlling for potential endogeneity could be a consequence of its coarseness, in the sense that *TC** is averaged at the county level and yet serves as a proxy for vehicle-use decisions made inherently at the household level (recall that *TC** is calculated as the total number of vehicle trips per day made in the region). In contrast, each weather variable is a non-averaged, relatively precise scientific measurement of a meteorological occurrence.

[21] Although of the expected signs, the coefficient estimates for *HUMIDITY*, *WIND*, and *HUMWIND* are not reported in Table 5 due to their statistical insignificance in these regressions – a likely consequence of the sample's relatively small size.

during which $PM_{2.5}$ concentrations are continuously increasing toward (and eventually reaching) a red air day episode in the region.

Despite Model 2's slightly better fit of the data overall (as evidenced by its lower AIC and BIC goodness-of-fit measures), we base the ensuing numerical analysis determining the Wasatch Front's optimal level of investment in preventative capital on Model 1, as this model controls for the potential existence of endogeneity present in our county-level trip count measure. Each of the covariates included in the model are evaluated at their respective mean values, except for *TC**, which, as we now reiterate in Section 7, is expressed as a constant-elasticity function of preventative capital stock N.

7. Estimates of the Wasatch Front's Optimal Preventative Capital Stock

We begin by calibrating (2) (our equation linking preventative capital stock $N(t)$ with daily trip counts $TC(t)$ within hazard function $\Psi(N(t), R(t))$, such that the (A,c) combinations are based upon $TC(t)$'s median daily value of approximately 175,000 trips within the region, as well as the rudimentary assumption concerning $N(t)$'s initial value of $20 million mentioned in Section 4. As in Acharya and Caplan (2019), we assume this value reflects both the human capital (e.g., prorated city and county employee time directed toward promoting preventative activities within the region, prorated salaries and wages of employees of nonprofit organizations such as Utah Physicians for a Healthy Environment (UPHE), the Wasatch Front Regional Council (WFRC), Breathe Utah, and Travelwise) and physical capital (infrastructure investments, including additional buses added to the region's fleet that are used specifically during the inversion season to increase ridership, additional route frequencies for Utah Transit Authority's (UTA's) light rail

system, TRAX, etc.).[22] Using (2), we obtain the resulting (A,c) combinations for the Wasatch Front presented in Table 6.

[INSERT TABLE 6 HERE]

We follow Berry et al. (2015) and Acharya and Caplan (2019) in assuming that exogenous background risk follows a logistic function. As mentioned in Section 6.3, Model 1 is our preferred specification for estimating hazard function $\Psi\big(N(t), R(t)\big)$, which is parameterized with the corresponding coefficient values contained in Table 5. The value for B is the Census Bureau's (2014) most recent estimate of the Wasatch Front's annual GDP. The value for J is then calculated as B net of average seasonal environmental damages (D) of $964 million associated with an average episodic outbreak in perpetuity. The estimate of $964 million is calculated using the Environmental Benefits Mapping and Analysis Program (BenMAP) (EPA, 2016a). This benefit is based on the assumption that, on average, a reduction of 29.3 percent in $PM_{2.5}$ concentration is required to attain the NAAQS of no greater than 35 μg/m³ per day during the inversion season in the Wasatch Front (Moscardini and Caplan, 2017).[23] Thus, as in Berry et al. (2015) and Acharya and Caplan (2019), our measure of J captures the present discounted stream of social net benefits in perpetuity that remains after an (average) outbreak has occurred during a given winter inversion season (relative to no outbreak having occurred).

[INSERT TABLE 7 HERE]

Our results for the Wasatch Front's optimal preventative capital stock, N^{ss}, along with corresponding optimal steady-state vehicle trip counts (denoted as TC^{ss}), are presented in Table 8. From this table we see that the value of the region's N^{ss} ranges from roughly $133 million to

[22] We have also run separate simulations assuming $N(t=0) = \$10$ million. Simulation results based on this assumption are included in the Appendix.
[23] For detailed information on the BenMAP facility visit https://www.epa.gov/benmap.

\$1.6 billion, depending upon the (A,c) combination. Corresponding amortized annual values of N^{ss} range from roughly \$11 million to \$129 million per year.[24] In column 5, a social deadweight loss (DWL) is applied to the Wasatch Front's respective annual investments in preventative capital reported in Table 8, reflecting both the region-wide social cost associated with raising revenue through the issuance of a regional bond, and the lost-consumer-surplus estimate of \$23.07 per vehicle-trip-reduced derived in Acharya and Caplan (2019).[25]

[INSERT TABLE 8 HERE]

Also shown in Table 8 is the extent to which the region's TC^{ss} decreases with trip count elasticity c, from approximately 145,000 trips per day (recall that our estimate for the Wasatch Front's current trips per day is roughly 175,000) to just under 2,200 as c rises from 0.1 to 1. Along with the monotonic decrease in TC^{ss} shown in the table, the corresponding values of N^{ss} exhibit a monotonically positive relationship with c. This latter finding differs from Acharya and Caplan's (2019) for Northern Utah, where N^{ss} reached its peak at $c = 0.8$.[26]

Corresponding percentage changes in optimal $PM_{2.5}$ concentrations (due to the monotonic decreases in TC^{ss}) are calculated via Monte Carlo simulation using Model 2 in Table 9. Both Models 1 and 2 in Table 9 control for potential endogeneity of TC using the weekday instruments described earlier in Section 6.3 (denoted TC^{*} here as well). However, Model 1 does so in the context of pooled OLS, while Model 2 also controls for fixed effects, which is the preferred model according to the standard Breusch-Pagan (1980) LM and Hausman (1978) χ^2

[24] A 5 percent interest rate and 20-year loan term period are assumed for the amortization exercise.
[25] See Acharya and Caplan (2019) for the full derivation of the per-trip-reduced DWL estimate. In addition, to account for the DWL associated with the issuance of a preventative-capital bond, we use the lower-bound DWL estimate of 20 percent (per dollar of revenue raised) reported in Campbell and Brown (2003). Campbell and Brown's (2003) estimate is in turn relatively conservative when compared with earlier DWL estimates reported in Findlay and Jones (1982), Freebairn (1995), Feldstein (1999), and Bates (2001).
[26] We nevertheless suspect that N^{ss} reaches its peak for the Wasatch Front at some value of $c > 1$.

tests for pooled-OLS vs. random effects and random vs. fixed effects models, respectively. For comparison purposes we present results from two additional models.

[INSERT TABLE 9 HERE]

In Model 3, $LagPM_{2.5}$ is removed in order to assess the impact on the remaining coefficients' signs and standard errors. Coefficient signs remain qualitatively similar across Models 1-3, as do their respective levels of statistical significance. However standard error estimates generally increase for each coefficient in Model 3, and the model's R^2 measure decreases by roughly 24 percent. Model 4 includes the second lag of $PM_{2.5}$ ($Lag_2PM_{2.5}$) in place of $LagPM_{2.5}$ as a control for the latter's potential endogeneity (Becketti, 2013). As with Model 3, coefficient signs and their significance levels remain qualitatively similar. Lastly, we note that the Wald χ^2 statistic is statistically significant for each model, indicating that we can reject the null hypothesis that the coefficients in each model are jointly statistically insignificant.[27]

Generally speaking the results in Table 9 are as expected. We obtain positive and statistically significant relationships between $PM_{2.5}$ concentrations, on the one hand, and TC^*, $LagPM_{2.5}$, *TEMP*, *SNOWDEPTH*, and *HUMIDITY* on the other. The relationships between $PM_{2.5}$ concentrations and *SNOWFALL* and *HUMWIND* are expectedly negative. The models' R^2 measures indicate relatively good fits for each model – the set of explanatory variables in Models 1 and 2 explaining roughly 70 percent of the daily variation in $PM_{2.5}$ concentrations.

Recall that the median trip count level for the Wasatch Front is roughly 175,000 trips per day. Hence, at the lowest trip-count elasticity assumed for this study of $c = 0.1$, an optimal preventative capital stock of approximately $133 million results in a concomitant 17 percent decrease in the region's TC^{ss}, specifically from 174,679 to 144,530 daily vehicle trips. At the

[27] Each model is estimated with White (1980) robust standard errors, which controls for potential within-panel autocorrelation (Arellano, 2003).

largest elasticity assumed in this study of $c = 1$, an optimized \$1.6 billion capital stock corresponds to a roughly 99 percent reduction in daily trip count.[28] Annualized health benefits associated with the concomitant decreases in $PM_{2.5}$ concentrations are calculated using BenMAP (EPA, 2016a). As anticipated, these benefits closely track the reductions in $PM_{2.5}$ concentrations. Social net benefits are then calculated as the respective differences between the annualized health benefits and the annual, amortized values of the steady-state preventative capital stock adjusted for deadweight loss. It is interesting to note that social net benefits also increase monotonically with trip count elasticity, indicating that the more responsive is trip count to investment in preventative capital, the larger the associated social net benefit associated with reduced $PM_{2.5}$ concentrations. Corresponding benefit-cost ratios range between 5.1:1 and 8.1:1.

As in Acharya and Caplan (2019), an important aspect of our trip-count results bears mention. The data upon which key functions in the numerical model are based, in particular the hazard function, implicitly link the Wasatch Front's $PM_{2.5}$ concentrations to the composition of the region's vehicle fleet during the period 2002 – 2012 in terms of vehicle models, ages, fuel-efficiencies, and emission-control technologies, etc. Thus, the optimal daily trip-count reductions derived here do not necessarily mean that trips themselves must decrease to those levels in today's terms. Rather, vehicle trips that produce emissions consistent with the fleet's composition during that time period (i.e., emissions-equivalent trips) must be reduced. Obviously, as more tier-three and zero-emission vehicles are included in the region's fleet over time, the magnitude of the reductions in vehicle trips necessary to meet the NAAQS threshold

[28] As noted in Acharya and Caplan (2019), a trip count this low would have to be obtained with a large percent of zero-emission vehicles included in the region's fleet. This finding is not unlike the California Public Utility Commission's recent estimation that seven million electric vehicles will need to be on the road in order for the state to meet its 2030 greenhouse gas reduction goals (Walton, 2018).

for $PM_{2.5}$ concentrations (i.e., the associated emissions-equivalent trips) will naturally decrease (Moscardini and Caplan, 2017).

Figure 5 presents a phase diagram corresponding to the dynamic system's steady-state equations (blue and grey lines) for the case of $z^{ss} \in (0, \infty)$), $c = 0.1$, and the parameter values and functional forms contained in Table 7. The steady-state equilibrium for this case occurs at the intersection of the two steady-state lines, corresponding to $N^{ss} = \$133$ million (from Table 8) and $R^{ss} = 12$ percent (from Table 3). The system's phase diagram indicates a saddle-path equilibrium, depicted by the teal-colored, arrowed line in the figure.

[INSERT FIGURE 5 HERE]

Lastly, as in Berry et al. (2015) and Acharya and Caplan (2019) we appeal to the law-of-motion equation for $\sigma(t)$ from Table 7 to explore the dynamics of increasing background risk over time and its effects on the Wasatch Front's optimal investment in preventative capital. Letting initial background risk be relatively close to zero (at the end of period 0), in particular $R(0) = 0.005$, and using $\sigma(t)$ to update $R(t)$ over time, background risk (at the end of) period 1 is given by $R(1) = R(0) + \sigma(0)$, where $\sigma(0) = R(0)(1 - \frac{R(0)}{0.12})$, and similarly for $R(2)$, $R(3)$ and so on. The corresponding $z(t)$ values are then calculated for given N^{ss} (we set $N^{\text{ss}} = \$133$ million for the analysis, which equals the N^{ss} value calculated from the simulation for $c = 0.1$), resulting in Figure 6 (y-axis is in billion \$). As indicated, investment for the initial period, $z(0)$, equals approximately \$118.5 million. The investment level for the subsequent period is $z(1) = \$$ 20.4 million, at which point the value of the preventative capital stock equals N^{ss}. Thus, for the remaining periods $z(t) = \delta N^{ss} = \$6.65$ million per period. Background risk continues increasing until reaching R^{ss} at the end of the eighth period.

[INSERT FIGURE 6 HERE]

8. Summary

This paper provides empirical estimates of the optimal investment in preventative capital to control episodic, wintertime, elevated $PM_{2.5}$ concentrations in Utah's Wasatch Front region, often rated as one of nation's worst air quality regions (ALA, 2017). We estimate a background risk of a red-air day occurring in the Wasatch Front during the winter inversion season of 12 percent, roughly 16 percent of the risk reported in Acharya and Caplan (2019) for Northern Utah. We also find a positive relationship between the aggregate number of daily vehicle trips taken in the region and the hazard associated with exceeding the NAAQS $PM_{2.5}$ concentration threshold of 35 $\mu g/m^3$ on an average winter day. Theoretically expected correlations between exceeding the threshold, on the one hand, and a host of unique weather variables, on the other, are also established. Unlike Acharya and Caplan's (2019) findings for background risk and the hazard associated with exceeding the NAAQS in Northern Utah, the determinants of these two risk measures in the Wasatch Front are potentially complicated by the GSL effect. We are able to leverage the weather control variables included in our dataset to (implicitly) isolate the GSL effect on $PM_{2.5}$ concentration levels in the Wasatch Front.

The value of Wasatch Front's optimal, steady-state preventative capital stock is estimated to range from $133 million to $1.6 billion, depending upon the assumed vehicle trip count elasticity with respect to investment in preventative capital. Further, we find that as the region's assumed trip-count elasticity rises the region's optimal daily vehicle trip count decreases monotonically from approximately 145,000 trips per day to just under 2,200. At the lowest trip-count elasticity assumed for this study the optimal preventative capital stock results in a concomitant 17 percent decrease in the region's vehicle trip count. The study's largest trip count elasticity corresponds to a 99 percent reduction in daily trip count. As expected, annual health benefits associated with the

concomitant decreases in $PM_{2.5}$ concentrations track the reductions quite closely. Social net benefits (which are positive for each scenario considered in this study) increase monotonically with trip count elasticity, indicating that the more responsive is vehicle trip count to investment in preventative capital, the larger the social net benefit. Corresponding benefit-cost ratios range between 5.1:1 and 8.1:1, which are larger than those reported in Acharya and Caplan (2019) for northern Utah, but still lower than the range estimated for the 1990 Clean Air Act Amendments in general (EPA, 2011).

Together with Acharya and Caplan (2019), this study is the first to consider optimal investments in preventative capital (e.g., via a municipal "clean air bond") to fund public investments in technologies capable of hastening more immediate mitigation of an episodic air pollution problem attributable primarily to mobile sources. Together the studies focus on two regions in the US with the ignominious reputations of having been ranked by the ALA (2017) as the nation's seventh (Wasatch Front) and eight (Northern Utah) worst air quality areas in terms of short-term particulate concentrations. The Wasatch Front and Northern Utah are therefore ideal locations within which to empirically assess potential market-based solutions to an episodic pollution problem; solutions such as investments in preventative capital and imposition of a seasonal gas tax à la Moscardini and Caplan (2017).

As mentioned in Acharya and Caplan (2019), in order to firm up our estimates of optimal investment in preventative capital to mitigate the health costs associated with episodic air pollution outbreaks, future study locations need to measure the impact on vehicle usage of varying levels of preventative capital stock over time, preferably at the household level. It would be useful to measure household-level behavioral responses to these investments from the perspective of more accurately calibrating the endogenous-risk numerical model we have used to

derive our social net benefit estimates, as well as from the perspective of simply learning the extent to which the investments induce both short- and longer-term changes in vehicle usage at the household level.

Appendix A

As trip-count elasticity, c, increases the corresponding preventative capital stocks associated with $N_0 = \$10$ million are everywhere lower than that associated with $N_0 = \$20$ million. The lower steady-state preventative capital stock, N^{ss}, values (in million \$) associated with the $N_0 = \$10$ million case are driven by the lower corresponding intercept, A, values for each c. Steady-state region-wide trip count, TC^{ss}, decreases monotonically with trip-count elasticity.

c	0.1	0.2	0.3	0.4	0.5	0.6	0.7	0.8	0.9	1
A	11.61	11.15	10.69	10.23	9.77	9.31	8.85	8.39	7.93	7.47
N^{ss}	135	290	465	657	854	1044	1213	1350	1,449	1,510
TC^{ss}	134,650	89,101	55,208	32,760	18,901	10,739	6,074	3,451	1,982	1,157

References

Acharya, R. and A.J. Caplan (2019) Optimal Vehicle Use in the Presence of Episodic Mobile-Source Air Pollution. *Resource and Energy Economics* 57, 185-204.

Alcott, T.I., W.J. Steenburgh, and N.F. Laird (2012) Great Salt Lake-effect precipitation: observed frequency, characteristics, and associated environmental factors. Weather and Forecasting 27(4), 954-971.

Alliance for a Better Utah (2017) Clean air caucus. Retrieved from the internet on July 17, 2017 at https://betterutah.org/clean-air-caucus/.

American Lung Association (ALA) (2017) State of the air. Retrieved from the Internet on June 12, 2017 at http://www.lung.org/our-initiatives/healthy-air/sota/city-rankings/most-polluted-cities.html.

American Public Transportation Association (APTA) (2014) Economic impact of public transportation investment, 2014 update. Retrieved from the internet on March 12, 2017 at https://www.apta.com/resources/reportsandpublications/Documents/Economic-Impact-Public-Transportation-Investment-APTA.pdf.

Anas, A. and R. Lindsey (2011) Reducing urban road transportation externalities: road pricing in theory and in practice. *Review of Environmental Economics and Policy* 5(1), 66-88.

Arellano, M. (2003) *Panel Data Econometrics*. Oxford: Oxford University Press.

Bachmann, J. (2007) Will the circle be unbroken: a history of the U.S. National Ambient Air Quality Standards. *Journal of the Air and Waste Management Association* 57, 652-697.

Barbier, E.B. (2013) Wealth accounting, ecological capital and ecosystem services. *Environment and Development Economics* 18(02), 133-161.

Bates, W. (2001) How much government? The effects of high government spending on economic performance. New Zealand Business Roundtable, Wellington.

Becketti, S. (2013) *Introduction to Time Series Using Stata*. College Station, TX: Stata Press.

Berry, K., Finnoff, D., Horan, R.D., and Shogren, J.F. (2015) Managing the endogenous risk of disease outbreaks with non-constant background risk. *Journal of Economic Dynamics & Control* 51,166-179.

Beevers, S.D. and D.C. Carslaw (2005) The impact of congestion charging on vehicle emissions in London. *Atmospheric Environment* 39(1), 1-5.

Breathe Utah (2017) Air Ware School Programs. Retrieved from the internet on September 28, 2017 at https://www.breatheutah.org/education/air-aware-school-programs.

Breusch, T. and A. Pagan (1980) The LM test and its applications to model specification in econometrics. *Review of Economic Studies* 47, 239-254.

Brookings institution (2017) A profile of Utah's Wasatch Front. Blueprint for American Prosperity. Metropolitan Policy Program. Retrieved from the internet on October 7, 2017 at https://www.brookings.edu/wp-content/uploads/2016/07/wasatch_font.pdf.

Button, K. and Verhoef, E. (1998) Road pricing, traffic congestion, and the environment. Edward Elgar Publishing: Northhampton, MA.

Campbell, H.F. and R.P.C Brown (2003) *Benefit-Cost Analysis*: *Financial and Economic Appraisal Using Spreadsheets*. Cambridge University Press, Melbourne.

Carnovale, M., and M. Gibson (2013) The effects of driving restrictions on air quality and driver behavior. UCSD Working Paper Series, Department of Economics, University of California, San Diego, Available at http://escholarship.org/uc/item/0v8813qm#page-1

Carpenter, D. M. (1993). The lake effect of the Great Salt Lake: overview and forecast problems. *Weather and Forecasting*, 8(2), 181-193.

Cleves, M., Gutierrez, R.G., Gould, W., Marchenko, Y.V. (2010) An introduction to survival analysis using Stata. College Station, TX: Stata Press.

Cropper, M. L., Jiang, Y., Alberini, A., and Baur, P. (2014) Getting cars off the road: the cost effectiveness of an episodic pollution control program. *Environmental and Resource Economics* 57, 117-143.

Cummings, R.G. and M.B. Walker (2000) Measuring the effectiveness of voluntary emission reduction programmes. *Applied Economics*, 32(13), 1719-1726.

Cutter, W.B. and M. Neidell (2009) Voluntary information programs and environmental regulation: evidence from "Spare the Air". *Journal of Environmental Economics and Management*, 58(3), 253-265.

DeShazo, J.R. (2016) Improving incentives for clean vehicle purchases in the United States: challenges and opportunities. *Review of Environmental Economics and Policy* 10(1), 149-165.

Dorsey, B. (2005) Mass transit trends and the role of unlimited access in transportation demand management. *Journal of Transport Geography* 13(3), 235-246.

Environmental Protection Agency (EPA), Office of Air and Radiation (2011) The benefits and costs of the clean air act from 1990 to 2020. Final Report – Rev.A. Retrieved from the internet on January 18, 2018 at https://www.epa.gov/sites/production/files/2015-07/documents/fullreport_rev_a.pdf.

Environmental Protection Agency (EPA) (2016a) Environmental Benefits Mapping and Analysis Program (BenMAP). Retrieved from the internet on January 4, 2016 at https://www.epa.gov/benmap.

Environmental Protection Agency (EPA) (2017) Nonattainment areas for criteria pollutants (green book). Retrieved from the internet on August 5, 2017 at https://www.epa.gov/green-book.

Environmental Public Health Tracking Program (EPHCP) (2017) Air Pollution and Public Health in Utah. Retrieved from the internet on September 16, 2017 at http://health.utah.gov/enviroepi/healthyhomes/epht/AirPollution_PublicHealth.pdf.

Ewing, R.H. (2008) Characteristics, causes, and effects of sprawl: a literature review. In *Urban Ecology: An International Perspective on the Interaction Between Humans and Nature*, pp. 519-535. Spring US. DOI: 10.1007/978-0-387-73412-5_34.

Feldstein, M. (1999) Tax avoidance and the deadweight loss of the income tax. *The review of Economics and Statistics* 81(4), 674-680.

Findlay, C. C. and R.L. Jones (1982) The marginal cost of Australian income taxation. *Economic Record* 58(162), 253.

Freebairn, J. (1995) Reconsidering the marginal welfare cost of taxation. *Economic Record* 71(213), 121–31.

Frondel, M., J. Peters, and C. Vance (2008) Identifying the rebound: evidence from a German household panel. *The Energy Journal* 29(4), 145-164.

Gallego, F., J.P. Montero, and C. Salas (2013) The effect of transport policies on car use: evidence from Latin American cities. *Journal of Public Economics*, 107, 47-62.

Gillies, R.R., S-Y Wang, and M.R. Booth (2010) Atmospheric scale interaction on wintertime Intermountain West low-level inversions. *Weather Forecasting* 25, 1196-1210.

Green Auto Market (GAM) (2016) What studies are finding: adoption of clean vehicle technologies will stay small-scale for now but we're likely approaching the cusp of change. Retrieved from the internet on October 7, 2017 at http://greenautomarket.com/studies-finding-adoption-clean-vehicle-technologies-will-stay-small-scale-now-likely-approaching-cusp-change/.

Greene, W. H. (2018) *Econometric Analysis* (Eighth Edition). New York: Prentice Hall.

Hausman, J. (1978) Specification test in econometrics. *Econometrica* 46, 1251-1271.

Henry, G.T. and C.S. Gordon (2003) Driving less for better air: impacts of a public information campaign. *Journal of Policy Analysis and Management*, 22(1): 45-63.

Horowitz, J.L. (1982) Air quality analysis for urban transportation planning. MIT Press: Cambridge, MA.

International Economic Development Council (IEDC) (2013) Creating the clean energy economy: analysis of the electric vehicle industry. Retrieved from the internet on September 10, 2017 at https://www.iedconline.org/clientuploads/Downloads/edrp/IEDC_Electric_Vehicle_Industry.pdf

J.D. Power and Associates (2010) Drive green 2020: more hope than reality? Special Report. Retrived from the internet on August 25, 2017 at http://businesscenter.jdpower.com/Corp/Store/DocumentDownload.aspx?PDFFile=10-All-DriveGreen2020-SR-sample.pdf.

Long, J.S. and J. Freese (2014) *Regression Models for Categorical Dependent Variables Using Stata* (Third Edition). College Station, TX: Stata Press.

Kassarjian, H.H. (1971) Incorporating ecology into marketing strategy: the case of air pollution. *Journal of Marketing* 35(3), 61-65.

Kotler, P. (2011) Reinventing marketing to manage the environmental imperative. *Journal of Marketing* 75(4), 132-135.

Litman, T. (2011) London congestion pricing: implications for other cities. Victoria Transport Policy Institute. Retrieved from the internet on March 22, 2017 at http://www.vtpi.org/london.pdf.

Litman, T. (2017) Evaluating public transit benefits and costs: best practices guidebook. Victoria Transport Policy Institute. Retrieved from the internet on March 24, 2017 at http://www.vtpi.org/tranben.pdf.

Moscardini, L.A., and Caplan A.J. (2017) Controlling episodic air pollution with a seasonal gas tax: the case of Cache Valley, Utah. *Environmental and Resource Economics* 66(4), 689-715.
Nesheli, M.M., A.Ceder, F. Ghavamirad, and S. Thacker (2017) Environmental impacts of public transport systems using real-time control method. *Transportation Research Part D: Transport and Environment* 51, 216-226.

Neuhaus, J.M., J.D. Kalbfleisch, and W.W. Hauck (1991) A comparison of cluster-specific and population-averaged approaches for analyzing correlated binary data. *International Statistical Review* 59, 25-35.

Osakwe, R. (2010) An analysis of the driving restriction implemented in San José, Costa Rica. Policy Brief, Environment for Development (EfD). Available at http://www.efdinitiative.org/publications/analysis-driving-restriction-implemented-san-jose-costa-rica.

Phang, S-Y and R.S. Toh (2004) Road congestion pricing in Singapore: 1975 to 2003. *Transportation Journal* 43 (2), 16-25.

Sierzchula, W., S. Bakker, K. Maat, and B. van Wee (2014) The influence of financial incentives and other socio-economic factors on electric vehicle adoption. *Energy Policy* 68, 183-194.

Silcox, G.D., K.E. Kelly, E.T. Crosman, C.D. Whiteman, and B.L. Allen (2012) Wintertime $PM_{2.5}$ concentrations during persistent, multi-day cold-air pools in a mountain valley. *Atmospheric Environment* 46, 17-24.

Sorrell, S., J. Dimitropoulos, M. Sommerville (2009) Empirical estimates of the direct rebound effect: a review. *Energy policy* 37, 1356-1371.

STATA (2017) What is the Difference Between Random-Effects and Population-Averaged Estimators. Retrieved from internet on October 4, 2017 at https://www.stata.com/support/faqs/statistics/random-effects-versus-population-averaged/

Steenburgh, J.W., S.F. Halvorson, and D.J. Onton (2000) Climatology of lake-effect snowstorms of the Great Salt Lake. *Monthly Weather Review* 128(3), 709-727.

TravelWise (2017). TravelWise to Keep Utah Moving. Retrieved from the internet on September 28, 2017 at https://travelwise.utah.gov.

Utah Climate Center (2016) Climate GIS|Station(s). Retrieved from the internet on March 20, 2017 at https://climate.usurf.usu.edu/mapGUI/mapGUI.php

Utah Department of Environment Quality (UDEQ) (2016a) Particulate Matter. Retrieved from internet on March 20, 2016 at http://www.deq.utah.gov/Pollutants/P/pm/Inversion.htm.

Utah Department of Environment Quality (UDEQ) (2016b) Information Sheet, p. 2. Retrieved from internet on March 10, 2016 http://www.deq.utah.gov/Topics/FactSheets/docs/handouts/pm25sipfs.pdf

Utah Department of Environment Quality (UDEQ) (2016c) Utah Air Monitoring Program. Retrieved from internet on March 10, 2016 at http://www.airmonitoring.utah.gov/network/Counties.htm

Utah Department of Environmental Quality (UDEQ) (2018) Inversions. Retrieved from the internet on January 11, 2018 at https://deq.utah.gov/Pollutants/P/pm/Inversion.htm.

Utah Department of Health (UDH) (2017) Air Pollution and Public Health in Utah, p. 21. Retrieved from internet on October 2, 2017 at http://health.utah.gov/enviroepi/healthyhomes/epht/AirPollution_PublicHealth.pdf.

Utah Division of Motor Vehicles (UDMV) (2017) Utah emissions testing. Retrieved from the internet on September 11, 2017 at https://www.dmv.com/ut/utah/emissions-testing.

Utah Department of Transportation (UDOT) (2014) Traffic statistics. Retrieved from the internet on August 26, 2014 at http://www.udot.utah.gov/main/f?p=100:pg::::1:T,V:507.

Utah Department of Transportation (UDOT) (2017) TravelWise: rethink your trip. Retrieved from the internet on August 23, 2017 at https://travelwise.utah.gov/about-us/.

Utah Economic Council (UEC) (2015) *Economic Report to the Governor*. Retrieved from the internet on August 7, 2015 at https://treasurer.utah.gov/wp-content/uploads/sites/10/2017/06/2015_erg.pdf.

Utah Physicians for a Healthy Environment (UPHE) (2017) Unmask my city. Retrieved from the internet on October 4, 2017 at http://uphe.org/priority-issues/unmask-my-city/.

United States Census (US Census) (2014) Quick Facts, Cache County Utah. Retrieved from the internet on March 17, 2015 at http://www.census.gov/quickfacts/table/RHI805210/49005

Walton, R. (2018) SoCal electric vehicle pilots focus on heavy duty, fleet uses. UtilityDive.com. Retrieved from the internet on January 14, 2018 at https://www.utilitydive.com/news/socal-edison-electric-vehicle-pilots-focus-on-heavy-duty-fleet-uses/514735/.

Wang, S.-Y. S., Hipps, L. E., Chung, O.-Y., Gillies, R. R., Martin, R. (2015) Long-term winter inversion properties in a mountain valley of the western United States and implications on air quality. *Journal of Applied Meteorology and Climatology*, 54, 2339-2352.

Wasatch Front Regional Council (WFRC) (2017) Final report summary. Wasatch Front Central Corridor Study. Retrieved from the internet on October 2, 2017 at http://wfccstudy.org//wp-content/uploads/2017/09/WFCCS_Final_Report_Summary_8_5x11_8_11_17-2.pdf.

Weather Underground (2016) About Our Data. Retrieved from the internet on March 6, 2016 at http://www.wunderground.com/about/data.asp.

White, H. (1980) A heteroskedasticity-consistent covariance matrix estimator and a direct test for heteroskedasticity. *Econometrica* 48, 817-838.

Whiteman, C.D., S.W. Hoch, J.D. Horel, and A. Charland (2014) Relationship between particulate air pollution and meterological variables in Utah's Salt Lake Valley. Atmospheric Environment 94, 742-753.

Wolff, H. (2014) Keep your clunker in the suburb: low emission zones and adoption of green vehicles. *The Economic Journal*, 124, F481-F512.

Zhang, W., C.-Y.C.L. Lawell, and V.I. Umanskaya (2016) The effects of license plate-based driving restrictions on air quality: theory and empirical evidence. Unpublished Working Paper. University of California at Davis. Retrieved from the internet on March 6, 2016 http://www.des.ucdavis.edu/faculty/Lin/driving_ban_paper.pdf.

Figure 1. Cache County (highlighted yellow) and Wasatch Front (highlighted red with breakout of specific counties).

Figure 2. Annual $PM_{2.5}$ concentrations in Salt Lake, Utah, and Weber Counties, various years.

Salt Lake County

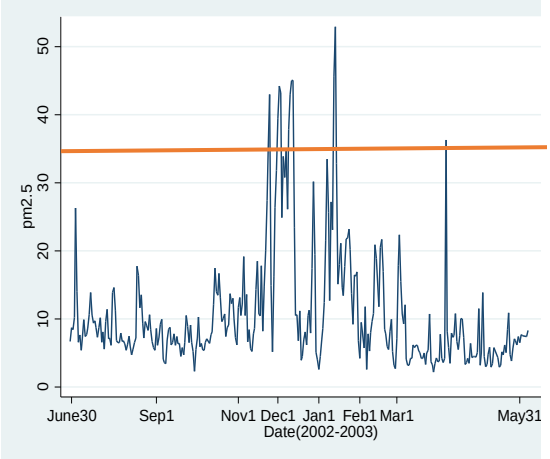

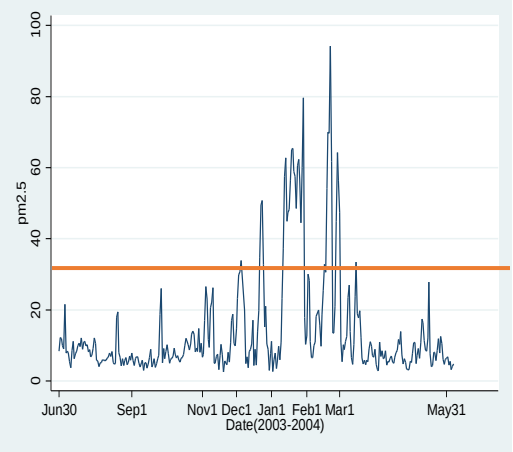

Utah County

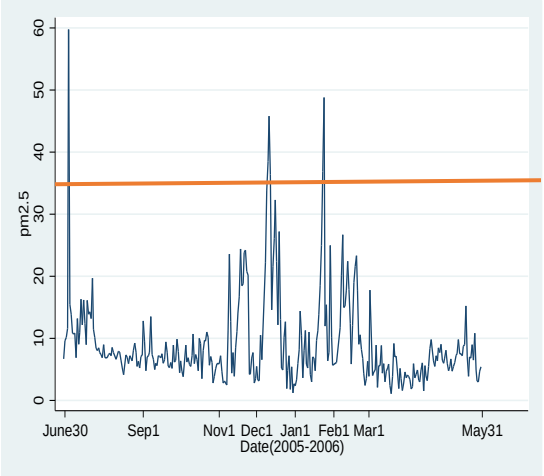

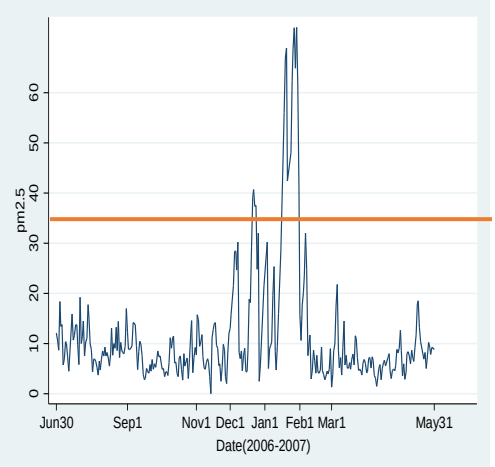

Weber County

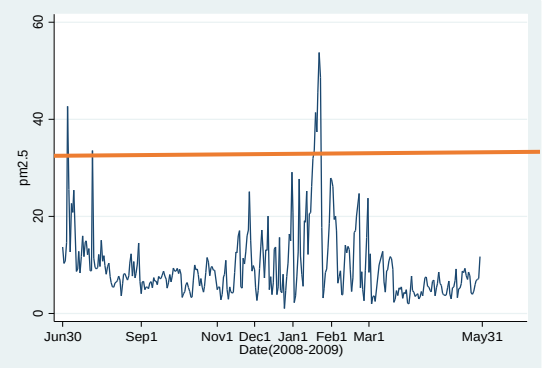

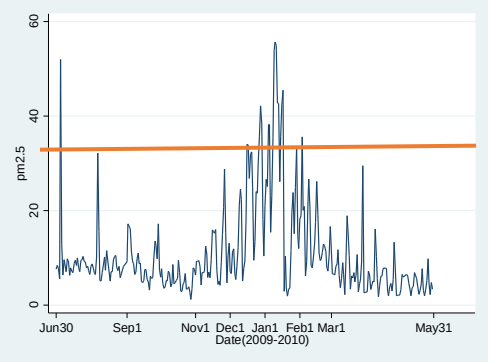

Figure 3. Monthly average PM 2.5 concentrations along the Wasatch Front for 2002 – 2012.

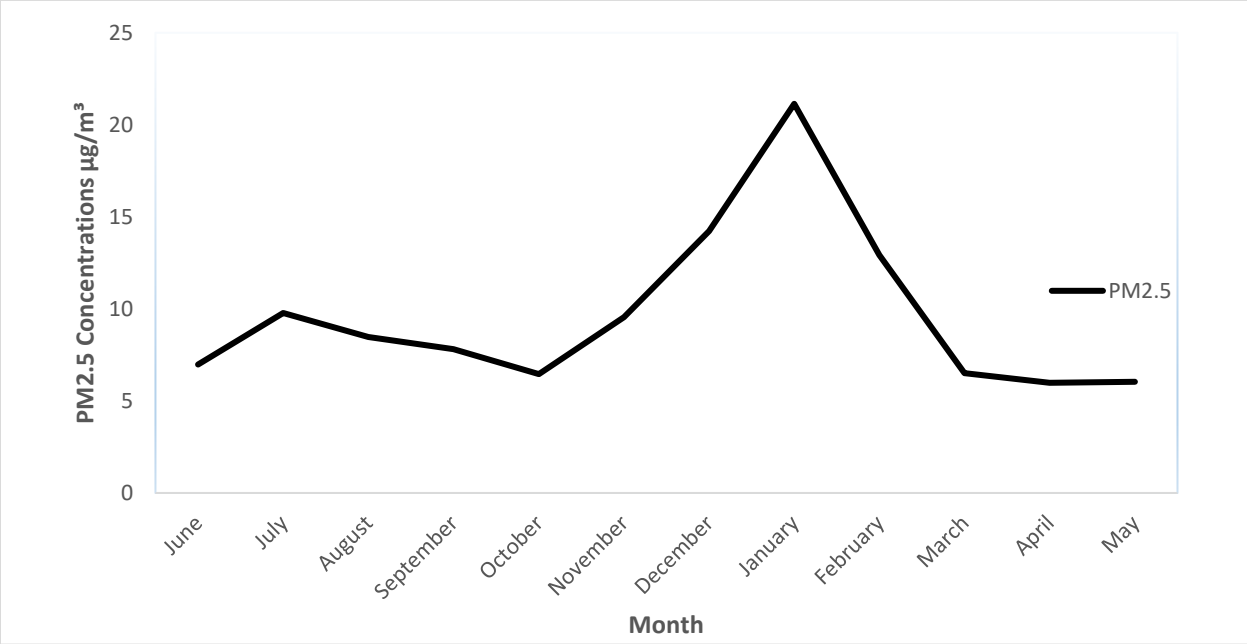

Figure 4. Winter inversion phenomenon in Utah's Wasatch Front region.

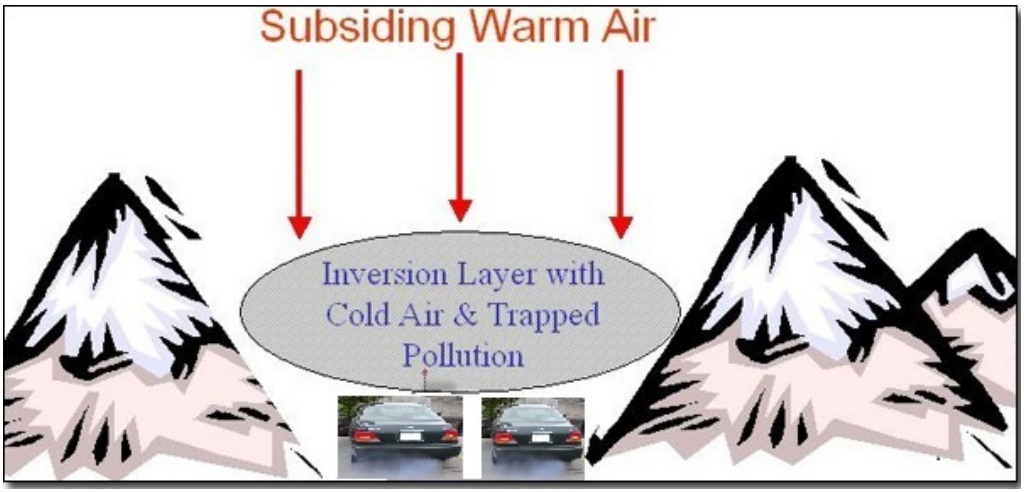

Figure 5. Phase diagram for a steady-state equilibrium.

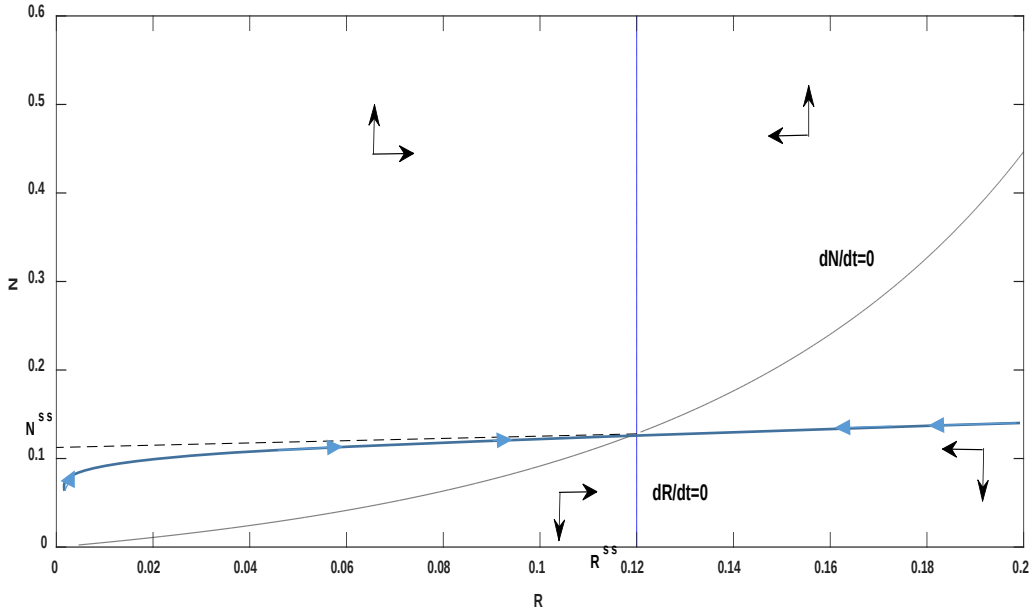

Figure 6. Time paths of $z(t)$ and $R(t)$ assuming increasing background risk over time.

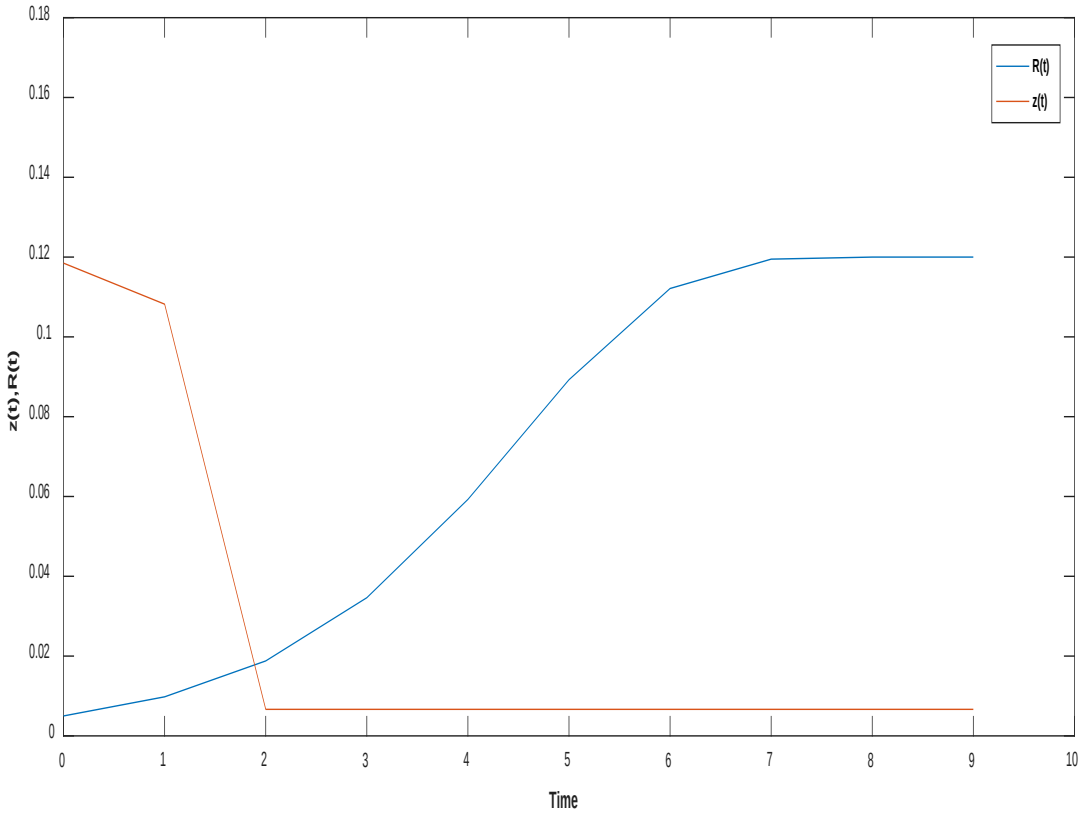

Table 1. Frequency of winter days in the Wasatch Front in which $PM_{2.5}$ concentrations exceeded the NAAQS.[a]

Year	Number of Winter Days Above 35 µg/m³	Percent of Winter Days Above 35 µg/m³
2002	24	27
2003	4	4
2004	33	36
2005	23	26
2006	12	13
2007	17	19
2008	10	11
2009	16	18
2010	16	18
2011	13	14
2012	0	0
Median[a]	16 (8.83)	18 (9.85)

[a]Percent of Winter days above 35 µg/m³ is based on the number of days for which $PM_{2.5}$ concentrations were recorded. We count a red air day in any of the three counties as a red air day for the entire region.
[b]Standard deviations are reported in parentheses.

Table 2. Variable definitions and summary statistics.[a]

Variable	Description	Mean[b] (SD)
TC	Daily trip count (# of vehicle trips).	174,679 (43,375.62)
$PM_{2.5}$	Daily $PM_{2.5}$ concentration ($\mu g/m^3$).	17.16 (14.88)
Y	=1 if daily $PM_{2.5}$ concentration is above 35 $\mu g/m^3$, 0 otherwise.	0.12 (0.32)
TEMP	Temperature gradient between mountain peak and valley floor (^0F).	0.21 (6.03)
WIND	Daily wind speed (miles/hour).	5.61 (3.63)
HUMIDITY	Daily humidity level (%).	74.09 (11.86)
SNOWFALL	Daily snowfall level (mm).	16.80 (41.37)
HUMWIND	HUMIDITY x WIND interaction term.	398.48 (245.12)
SNOWDEPTH	Daily snow depth (mm).	133.65 (218.56)

a Standard deviations are in parentheses.
[b] *TC* is the median daily trip count for the Wasatch Front region (summed across Salt Lake, Utah, and Weber Counties).

Table 3. Population-averaged probit regression results.[a]

Variable	Coefficients (SE)	Marginal Effects (SE)
$LagPM_{2.5}$	0.065*** (0.007)	0.006*** (0.001)
TEMP	0.01 (0.01)	0.001 (0.001)
HUMIDITY	0.01 (0.012)	0.001 (0.001)
HUMWIND	-0.002** (0.001)	-0.0002** (0.0001)
SNOWFALL	-0.01*** (0.003)	-0.001** (0.0004)
SNOWDEPTH	0.0001 (0.0003)	0.00001 (0.00003)
R^{ss} (Wasatch Front)	12%	---
R^{ss} (Salt Lake County)	11%	
R^{ss} (Utah County)	14%	
R^{ss} (Weber County)	10%	
Predicted red air day = 1 Observed red air day = 1	57%	---
Predicted red air day = 0 Observed red air day = 0	98%	---
Number of observations	1,648	---

[a] Robust standard errors are in parentheses.
***, ** and * indicate significance at 1, 5 and 10% levels, respectively.

Table 4. Panel regression results for the Great Salt Lake effect ($PM_{2.5}$ is dependent variable).[a]

Variable	Coefficients (S.E.)	
	Model 1	**Model 2**
LagPM2.5	0.439*** (0.044)	0.421*** (0.010)
*TC**	0.138*** (0.017)	0.129*** (0.005)
Yr_T	-0.021*** (0.007)	-0.022*** (0.006)
TEMP	0.068*** (0.009)	0.070*** (0.012)
SNOWFALL	-0.001*** (0.0002)	-0.001*** (0.00008)
SNOWDEPTH	0.0002*** (0.00002)	0.0002*** (0.00008)
HUMIDITY	0.012*** (0.002)	0.016*** (0.001)
WIND	0.057*** (0.008)	0.055*** (0.010)
HUMWIND	-0.002*** (0.0003)	-0.002*** (0.0002)
SNOWFALL_TEMP	-0.0002*** (0.00003)	-0.0002*** (0.000003)
TEMP_HUMIDITY	-0.0005*** (0.0001)	-0.0005*** (0.0001)
SLC	0.758*** (0.212)	0.806*** (0.246)
SLC_TEMP	-0.047*** (0.008)	-0.042*** (0.013)
SLC_SNOWFALL	-0.004*** (0.0002)	-0.004*** (0.0001)
SLC_SNOWDEPTH	0.001*** (0.00003)	0.001*** (0.00007)
SLC_HUMIDITY	-0.003* (0.001)	-0.003 (0.002)
SLC_WIND	-0.049*** (0.007)	-0.041*** (0.012)
SLC_HUMWIND	0.00001 (0.0003)	-0.0002 (0.0002)
SLC_TEMP_SNOWFALL	0.00003 (0.00004)	0.00008*** (0.00001)
SLC_TEMP_HUMIDITY	0.0004*** (0.00009)	0.0004** (0.0001)
R^2 (overall)	0.73	0.73
Wald χ^2	457.9***	3297.61***
Number of Observations	1,643	1,594

[a] Robust standard errors in parentheses

***, ** and * indicate significance at 1, 5 and 10% levels, respectively.

Table 5. Panel survival regression results.[a]

Variable	Coefficients (S.E.)	
	Model 1	**Model 2**
TC[*]	0.40	0.63**
	(0.4)	(0.27)
TEMP	0.063***	0.06***
	(0.02)	(0.02)
SNOWDEPTH	-0.0005	-0.0003
	(0.0006)	(0.001)
SNOWFALL	-0.011**	-0.011**
	(0.005)	(0.004)
AIC	320.962	316.187
BIC	327.477	322.702
ln_*p*	0.710	0.72
	(0.072)	(0.06)
Number of observations	192	192

[a] Robust standard errors are in parentheses.
***, ** and * indicate statistical significance at 1, 5 and 10% levels, respectively.

Table 6. (A, c) combinations used in the numerical analysis.

c	0.1	0.2	0.3	0.4	0.5	0.6	0.7	0.8	0.9	1.0
A	11.68	11.29	10.90	10.51	10.11	9.72	9.33	8.94	8.55	8.16

Table 7. Parameter values and functional forms for the numerical analysis.

Parameter	Functional form/value	Source
R^{**}	12%	Probit analysis (Section 6.1)
$\sigma(t)$	$R(t)(1-\frac{R(t)}{R^{ss}})$	Berry et al. (2015) Acharya and Caplan (2019)
$\Psi\big(N(t),R(t)\big)$	$R(t)\mathrm{p}t^{p-1}\ exp(\boldsymbol{\beta X}(t)')$	Survival analysis (Section 5.2)
δ	0.05	Berry et al. (2015) Acharya and Caplan (2019)
r	0.03	Berry et al. (2015) Acharya and Caplan (2019)
B	\$ 47.36 billion	U. S. Census Bureau (2014)
D	\$964 million	BenMAP (EPA, 2016)
J	\$ 1.55 trillion	$=\frac{B-D}{r}$
TC	$=exp(A-c\log(N))$	Acharya and Caplan (2019)

Table 8. Estimated N^{ss} values (million $), associated TC^{ss} (daily region-wide vehicle trips), and social net benefit (million $).

c	A	N^{ss}	Annual N^{ss}	Annual N^{ss} + DWL	TC^{ss}	% Change in PM2.5	Annual Benefit	Social Net Benefit	Benefit-Cost Ratio
0.1	11.68	133	10.67	13.50	144,530	2.12	69.3	55.80	5.13
0.2	11.29	282.1	22.64	28.13	102,888	5.82	189.22	161.09	6.73
0.3	10.90	449.9	36.10	44.11	68,646	10.04	326.01	281.90	7.39
0.4	10.51	634.3	50.90	61.65	43,826	14.5	468.39	406.74	7.60
0.5	10.11	829.8	66.59	80.29	27,119	16.02	613.13	532.84	7.64
0.6	9.72	1,025.2	82.26	98.96	16,458	23.48	755.47	656.51	7.63
0.7	9.33	1,210.1	97.10	116.67	9,885	27.77	893.48	776.81	7.66
0.8	8.94	1,373.7	110.23	132.37	5,926	31.84	1022.72	890.35	7.73
0.9	8.55	1,508.1	121.01	145.27	3,569	35.64	1144.44	999.17	7.88
1	8.16	1,609	129.11	154.96	2,171	39.16	1254.79	1,099.83	8.10

Table 9. Regression results for Monte Carlo Simulation ($PM_{2.5}$ is dependent variable).[a]

Variable	Coefficients (S.E.)			
	Model 1	**Model 2**	**Model 3**	**Model 4**
*TC**	0.13*** (0.02)	0.11*** (0.03)	0.14** (0.06)	0.13*** (0.04)
$LagPM_{2.5}$	0.03*** (0.001)	0.02*** (0.001)	---	---
$Lag_2PM_{2.5}$	---	---	---	0.01*** (0.0007)
TEMP	0.02** (0.008)	0.02*** (0.008)	0.04*** (0.006)	0.03*** (0.006)
SNOWDEPTH	0.0002** (0.00005)	0.0004*** (0.0001)	0.0003* (0.0002)	0.0004** (0.0002)
SNOWFALL	-0.003** (0.0008)	-0.002*** (0.0009)	-0.004*** (0.001)	-0.003*** (0.001)
HUMIDITY	0.007*** (0.001)	0.01*** (0.001)	0.02*** (0.004)	0.01*** (0.003)
WIND	-0.04*** (0.009)	-0.03** (0.01)	-0.01 (0.02)	-0.02 (0.02)
HUMWIND	-0.001* (0.0003)	-0.001 (0.0005)	-0.001* (0.0007)	-0.001 (0.0007)
$\chi 2$ (Wald)	42.08***	29.73***	9.04***	40.38***
R^2	66.48	65.44	50.00	56.19
Number of observations	1643	1643	1835	1615

[a] Robust standard errors in parentheses

***, ** and * indicate significance at 1, 5 and 10% levels, respectively.